2. EXPLANATORY NOTES[1]

Shipboard Scientific Party[2]

INTRODUCTION

Standard procedures for both drilling operations and preliminary shipboard analysis of the material recovered during the Deep Sea Drilling Project (DSDP) and the Ocean Drilling Program (ODP) have been amended regularly and upgraded since drilling began in 1968. In this chapter, we have assembled information that will help the reader to understand the basis for our preliminary conclusions and also help the interested investigator to select samples for further analysis. This information concerns only shipboard operations and analyses described in the site reports in the *Initial Reports* volume of the Leg 125 *Proceedings of the Ocean Drilling Program.* Methods used by various investigators for shorebased analysis of Leg 125 data will be described in the individual scientific contributions published in the *Scientific Results* volume of the *Proceedings of the Ocean Drilling Program.*

Authorship of Site Chapters

The separate sections of each site chapter were written by the following shipboard scientists (authors are listed in alphabetical order in parentheses, no seniority is implied):

Principal Results: Fryer, Pearce
Background and Scientific Objectives: Fryer, Pearce
Operations: Pettigrew, Stokking
Lithostratigraphy: Haggerty, Heling, McCoy, Rigsby
Biostratigraphy: Ciampo, Milner, Stabell, Xu
Igneous and Metamorphic Petrology: Arculus, Johnson, Ishii, Maekawa, Murton, Saboda, van der Laan
Igneous and Metamorphic Geochemistry: Arculus, Johnson, Ishii, Maekawa, Murton, Saboda, van der Laan
Sediment/Fluid Geochemistry: Mottl
Structural Studies: Lagabrielle, Phipps
Paleomagnetism: Ali, Haston, Stokking
Sediment-Accumulation Rates: Ali, Ciampo, Stabell
Physical Properties: Ballotti, Burke, Marlow
Downhole Measurements: Hobart, Marlow
Summary and Conclusions: Fryer, Pearce, Stokking

Following the text of each site chapter are summary core descriptions ("barrel sheets" and igneous-rock visual core descriptions) and photographs of each core.

Survey Data

Survey data collected prior to Leg 125 and used in the site selection process are discussed in Fryer et al. and Horine et al. (this volume). The underway geophysical data collected aboard *JOIDES Resolution* during Leg 125 are discussed in a separate "Underway Geophysics" chapter (this volume). The underway data include bathymetry, magnetics, and seismic-reflection profiles.

Drilling Characteristics

Water circulation down the hole is open, hence cuttings are lost onto the seafloor and cannot be examined. The only available information about sedimentary stratification in uncored or unrecovered intervals, other than from seismic data or wireline-logging results, is from an examination of the behavior of the drill string as observed and recorded on the drilling platform. Typically, the harder a layer, the slower and more difficult it is to penetrate. A number of other factors, however, determine the rate of penetration, so it is not always possible to relate drilling time directly to the hardness of the layers. Bit weight and revolutions per minute, recorded on the drilling recorder, influence the penetration rate.

Drilling Deformation

When cores are split, many show signs of significant sediment disturbance, including the concave-downward appearance of originally horizontal bands, haphazard mixing of lumps of different lithologies (mainly at the tops of cores), and the near-fluid state of some sediments recovered from tens to hundreds of meters below the seafloor. Core deformation probably occurs during any of several steps in which the core may experience stresses sufficient to alter its physical characteristics: cutting, retrieval (with accompanying changes in pressure and temperature), and core handling on deck.

Shipboard Scientific Procedures

Numbering of Sites, Holes, Cores, Sections, and Samples

ODP drill sites are numbered consecutively from the first site drilled by the *Glomar Challenger* in 1968. A site number refers to one or more holes drilled while the ship was positioned over one acoustic beacon. Multiple holes may be drilled at a single site by pulling the drill pipe above the seafloor (out of the hole), moving the ship some distance from the previous hole, and then drilling another hole.

For all ODP drill sites, a letter suffix distinguishes each hole drilled at the same site. For example, the first hole drilled is assigned the site number modified by the suffix *A*, the second hole takes the site number and suffix *B*, and so forth. Note that this procedure differs slightly from that used by DSDP (Sites 1 through 624), but prevents ambiguity between site- and hole-number designations. It is important, for sampling purposes, to distinguish among holes drilled at a site, because recovered sediments or rocks from different holes usually do not come from equivalent positions in the stratigraphic column.

The cored interval is measured in meters below seafloor (mbsf). The depth interval assigned to an individual core begins with the depth below the seafloor where coring began and extends to the depth where coring ended (see Fig. 1). For example, each coring interval is generally up to 9.5 m long,

[1] Fryer, P., Pearce, J. A., Stokking, L. B., et al., 1990. *Proc. ODP, Init. Repts.*, 125: College Station, TX (Ocean Drilling Program).
[2] Shipboard Scientific Party is as given in the list of participants preceding the contents.

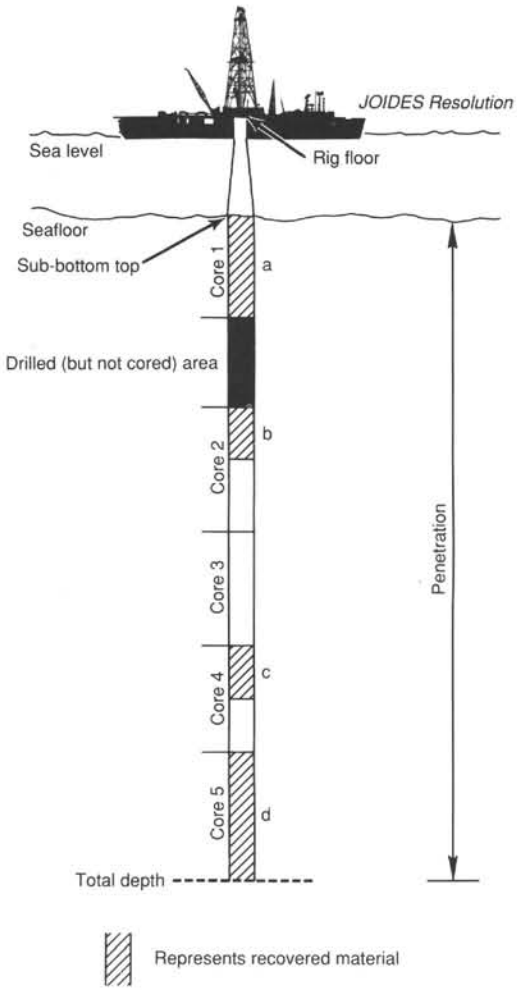

Bottom felt: distance from rig floor to seafloor (number written on the white board).
Total depth: distance from rig floor to the bottom of the hole.
Penetration: distance from seafloor to the bottom of the hole.
Number of cores: total of all cores recorded, including cores with no recovery.
Total length of cored section: distance from sub-bottom top to total depth minus drilled (but not cored) areas in between.
Total core recovered: total from adding a, b, c, and d in the diagram.
Core recovery (%): equals TOTAL CORE RECOVERED divided by TOTAL LENGTH OF CORED SECTION times 100 (See Fig. 2, "Explanatory notes", *Proc. ODP, Init. Repts.*, Vol. 122).

Figure 1. Coring and depth intervals.

which is the length of a core barrel. Coring intervals may be shorter and may not necessarily be adjacent, if separated by drilled intervals. In soft sediments, the drill string can be "washed ahead" with the core barrel in place, without recovering sediments. This is achieved by pumping water down the pipe at high pressure to wash the sediment out of the way of the bit and up the space between the drill pipe and the wall of the hole. If thin, hard rock layers are present, then it is possible to get "spotty" sampling of these resistant layers within the washed interval, and thus to have a cored interval greater than 9.5 m. When drilling hard rock, a center bit may replace the core barrel if it is necessary to drill without core recovery.

Cores taken from a hole are numbered serially from the top of the hole downward. Core numbers and their associated cored intervals in meters below seafloor usually are unique in

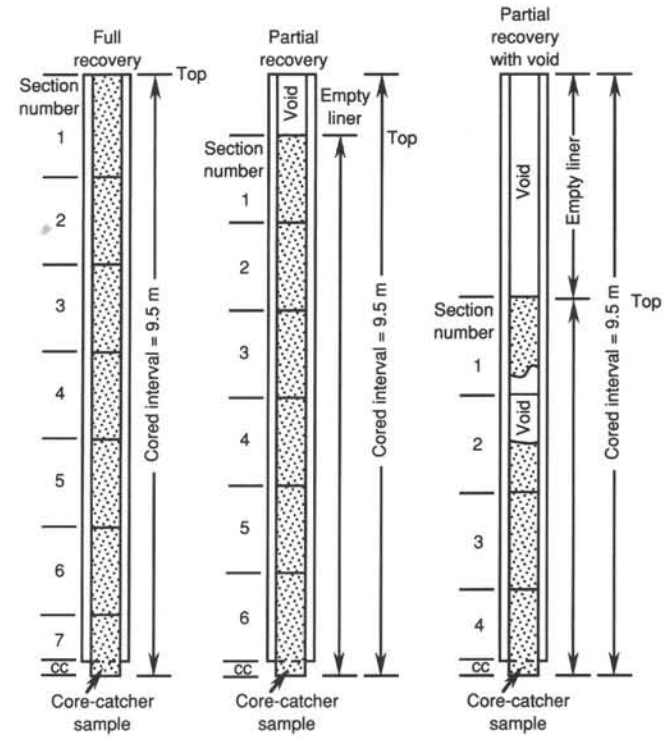

Figure 2. Examples of numbered core sections.

a given hole; however, this may not be true if an interval must be cored twice, because of caving of cuttings or other hole problems. Maximum full recovery for a single core is 9.5 m of rock or sediment contained in a plastic liner (6.6-cm internal diameter) plus about 0.2 m (without a plastic liner) in the core catcher (Fig. 2). The core catcher is a device at the bottom of the core barrel that prevents the core from sliding out while the barrel is being retrieved from the hole. In certain situations (e.g., when coring gas-charged sediments that expand while being brought on deck) recovery may exceed the 9.5-m maximum.

A recovered core is divided into 1.5-m sections that are numbered serially from the top (Fig. 2). When full recovery is obtained, the sections are numbered from 1 through 7 (the last section may be shorter than 1.5 m, and, rarely, an unusually long core may require more than seven sections). When less than full recovery is obtained, there will be as many sections as needed to accommodate the length of the core recovered; for example, 4 m of core would be divided into two 1.5-m sections and a 1-m section. If cores are fragmented (recovery less than 100%), sections are numbered serially and intervening sections are noted as void, whether shipboard scientists believe that the fragments were contiguously *in situ* or not. In rare cases, a section less than 1.5 m may be cut to preserve features of interest (e.g., lithological contacts).

By convention, material recovered from the core catcher is placed below the last section when the core is described and labeled core catcher (CC); in sedimentary cores, this material is treated as a separate section. The core catcher is placed at the top of the cored interval in cases where material is recovered only in the core catcher. However, information supplied by the drillers or by other sources may permit more precise interpretation of the correct position of core-catcher material within an incompletely recovered cored interval.

A recovered rock (basalt, gabbro, peridotite, or serpentinite) core is also cut into 1.5-m sections that are numbered serially; however, each piece of rock is then assigned a

number. Fragments of a single piece are assigned a single number, and individual fragments are identified alphabetically. The core-catcher sample is placed at the bottom of the last section and is treated as part of the last section, rather than as a separate section. Scientists completing visual core descriptions describe each lithologic unit, noting core and section boundaries only as physical reference points.

When, as is usually the case, the recovered core is shorter than the cored interval, by convention, the top of the core is equated with the top of the cored interval to achieve consistency in handling the analytical data derived from the cores. Samples removed from the cores are designated by the distance measured in centimeters from the top of the section to the top and bottom of each sample removed from that section. In curated hard-rock sections, sturdy plastic spacers are placed between pieces that did not fit together to protect them from damage in transit and in storage; therefore, the centimeter interval noted for a hard-rock sample has no direct relationship to the depth of that sample within the cored interval, but is only a physical reference to the location of the sample within the curated core.

A full identification number for a sample consists of the following information: leg, site, hole, core number, core type, section number, piece number (for hard rock), and interval in centimeters measured from the top of section. For example, a sample identification of "125-778A-10R-1, 10–12 cm" would be interpreted as representing a sample removed from the interval between 10 and 12 cm below the top of Section 1, Core 10 (R designates that this core was taken with the rotary core barrel) of Hole 778A during Leg 125.

All ODP core and sample identifiers indicate core type. The following abbreviations are used: R = rotary core barrel (RCB); H = hydraulic piston core (HPC; also referred to as APC, or advanced hydraulic piston core); P = pressure core barrel; X = extended core barrel (XCB); B = drill-bit recovery; C = center-bit recovery; I = *in-situ* water sample; S = sidewall sample; W = wash-core recovery; and M = miscellaneous material. APC, XCB, and RCB cores were cut during Leg 125.

Core Handling

Sediments

As soon as a core has been retrieved on deck, a sample is taken from the core catcher and taken to the paleontological laboratory for an initial age assessment. The core is then placed on the long horizontal rack, and gas samples may be taken by piercing the core liner and withdrawing gas into a vacuum tube. Voids within the core are sought as sites for gas sampling. Some of the gas samples are stored for shorebased study, but others are analyzed immediately as part of the shipboard safety and pollution-prevention program. Next, the core is marked into section lengths, each section is labeled, and the core is cut into sections. Interstitial-water (IW) and organic geochemistry (OG) samples are then taken. In addition, some headspace gas samples are scraped from the ends of cut sections on the catwalk and sealed in glass vials for light hydrocarbon analysis. Each section is then sealed at the top and bottom by gluing on color-coded plastic caps: blue to identify the top of a section and clear for the bottom. A yellow cap is placed on section ends from which a whole-round sample has been removed. The caps are usually attached to the liner by coating the end of the liner and the inside rim of the cap with acetone, and then the caps are taped to the liners.

These cores then are carried into the laboratory, where the sections are again labeled, using an engraver to mark permanently the full designation of the section. The length of the core in each section and the core-catcher sample are measured to the nearest centimeter; this information is logged into the shipboard CORELOG data-base program.

Next, the whole-round sections from APC and XCB cores are run through the multisensor track (MST). This includes the GRAPE (gamma-ray attenuation porosity evaluator) and *P*-wave logger devices, which measure the bulk density, porosity, and sonic velocity, and also includes a meter that determines the volume magnetic susceptibility. After the core has equilibrated to room temperature (approximately 3 hr), thermal conductivities are measured, and the cores are split.

Cores of relatively soft material are split lengthwise into working and archive halves. The softer cores are split with a wire or saw, depending on the degree of induration. Harder cores are split with a band saw or diamond saw. Because cores during Leg 125 were split with wire from the bottom to top, older material may have been transported up the core on the split face of each section. Thus, one should be aware that the very near-surface part of the split core might be contaminated.

The working half is sampled for both shipboard and shorebased laboratory studies. Each extracted sample is logged into the sampling computer data-base program by its location and name of the investigator receiving the sample. Records of all removed samples are kept by the ODP curator. The samples are sealed in plastic vials or bags and labeled. Samples are routinely taken for analyzing shipboard physical properties. These samples are then used to determine calcium carbonate contents (coulometric analysis), and these data are reported in site chapters.

The archive half is described visually. Smear slides are made from samples taken from the archive half and are supplemented by thin sections taken from the working half. Sections from the archive half that do not show evidence of drilling disturbance are measured in the cryogenic magnetometer. The archive half is then photographed with both black-and-white and color film, a core at a time. Close-up photographs (black-and-white) are taken of particular features for illustrations.

Both halves of the core are then placed into labeled plastic tubes, sealed, and transferred to cold-storage space aboard the drilling vessel. At the end of the leg, the cores are transferred from the ship in refrigerated air-freight containers to cold storage at the Gulf Coast Repository at the Ocean Drilling Program, Texas A&M University, College Station, Texas.

Igneous and Metamorphic Rocks

Igneous and metamorphic rock cores are handled differently from sedimentary cores. Once on deck, the core catcher is placed at the bottom of the core liner, and total core recovery is calculated by shunting the rock pieces together and measuring to the nearest centimeter; this information is logged into the shipboard CORELOG data-base program. The core is then cut into 1.5-m-long sections and transferred into the laboratory.

The contents of each section are transferred into 1.5-m-long sections of split core liner, where the bottom of oriented pieces (i.e., pieces that clearly could not have rotated top to bottom about a horizontal axis in the liner) are marked with a red wax pencil. This is to ensure that orientation is not lost during splitting and labeling. The core is then split into archive and working halves. A plastic spacer is used to separate individual pieces, and/or reconstructed groups of pieces, in the core liner. These spacers may represent a

substantial interval of no recovery. Each piece is numbered sequentially from the top of each section, beginning with number 1; reconstructed groups of pieces are assigned the same number, but are lettered consecutively. Pieces are labeled on the rounded, not sawn, surfaces. If the piece is oriented, an arrow is added to the label pointing to the top of the section.

The working half is sampled for shipboard laboratory studies. Records of all samples are kept by the curator at ODP. Minicore samples are routinely taken for physical-properties and magnetic studies. Some of these samples are later subdivided for X-ray fluorescence (XRF) analysis and thin-sectioning, so that as many measurements as possible are performed using the same pieces of rock. At least one minicore is taken per lithologic unit when recovery permits, generally from the freshest areas of core. Additional thin sections, X-ray-diffraction (XRD) samples, and XRF samples are selected from areas of particular interest. Samples for shorebased studies are selected in a sampling party held after drilling has ended.

The archive half is described visually, then photographed with both black-and-white and color film, one core at a time. Both halves of the core are then shrink-wrapped in plastic to prevent rock pieces from vibrating out of sequence during transit, placed into labeled plastic tubes, sealed, and transferred to cold-storage space aboard the drilling vessel.

SEDIMENT CORE DESCRIPTION FORMS

Sediments and Sedimentary Rocks

Visual core descriptions, smear slide and thin-section descriptions, $CaCO_3$ concentrations, and biostratigraphic criteria provide the shipboard data for core descriptions in this volume. Core description forms (Fig. 3) summarize these data and also indicate sample locations in the core. This information represents field notes taken on board ship under time constraints. In some cases, changes are made on the basis of post-cruise findings. However, production schedules prohibit modification of the core description forms with subsequent findings; therefore, occasional ambiguities or discrepancies may be present.

Core Designation

Cores are designated using leg, site, hole, core number, and core type as previously discussed (see "Numbering of Sites, Holes, Cores, Sections, and Samples" section, this chapter). In addition, the cored interval is specified in terms of meters below sea level (mbsl) and meters below seafloor (mbsf). On the basis of drill-pipe measurements (dpm), as reported by the SEDCO coring technician and the ODP operations superintendent, depths are corrected for the height above sea level of the dual elevator stool on the rig floor to give true water depth and the correct interval (mbsl).

Age Data

Abundance of microfossils, their preservation, and zone assignment, as determined by shipboard paleontologists, appear on the core-description form under the heading "Biostratigraphic Zone/Fossil Character." The geologic age determined from paleontological and/or paleomagnetic results is shown in the "Time-Rock Unit" column.

Calcareous nannofossils and planktonic foraminifers provided most of the age determinations in the forearc basin sites. Diatom biostratigraphy is critical on the seamount sites located beneath the carbonate compensation depth (CCD). Detailed information about zonations and terms used to report abundance and preservation is presented in the "Biostratigraphy" section (this chapter).

Paleomagnetic, Physical-Properties, and Chemical Data

Columns are provided on the core description form for recording paleomagnetic results, physical-properties values (wet-bulk density, porosity, and compressional-wave velocity) and chemical data (percentage of $CaCO_3$ determined by coulometric analysis, and total organic carbon calculated by difference between total carbon from nitrogen-carbon-sulfur (NCS) analysis and inorganic carbon from coulometric analysis. Additional information about shipboard procedures for collecting these types of data is found in "Paleomagnetism," "Physical Properties," and "Inorganic Geochemistry" sections (this chapter).

Graphic Lithology Column

The lithology of the recovered material is represented on the core description forms by a single symbol or by a group of two or more symbols (Fig. 4) in the column titled "Graphic Lithology." The symbols in a group correspond to end members of sediment constituents, such as clay or nannofossil ooze. For example, sediment composed of 20% nannofossils and 80% clay would be represented by the symbol for nannofossil ooze in 20% of the column and the symbol for clay in the remaining 80% of the column. Where different types of sediment are finely interbedded, symbols given in the column are schematic because the scale of the core description forms does not permit an accurate representation.

Some cores recovered during Leg 125 have intercalations of sedimentary material, as well as serpentine and serpentinite associated with igneous and metamorphic rocks. Intervals described by igneous and metamorphic petrologists are indicated by the symbol "IM" (see "Hard-Rock Core Description Forms" section, this chapter).

Sediment Disturbance

The coring technique, which uses a 25-cm-diameter bit with a 6-cm-diameter core opening, may result in varying degrees of mechanical disturbance of recovered core material. This is illustrated in the "Drilling Disturbance" column on the core description form (using the symbols in Fig. 5). Blank regions indicate a lack of drilling disturbance. Drilling disturbance is recognized for soft and firm sediments using these categories:

1. Slightly deformed: bedding contacts are slightly bent.
2. Moderately deformed: bedding contacts have undergone extreme bowing.
3. Highly deformed: bedding is completely disturbed, sometimes showing symmetrical diapirlike or flow structures.
4. Soupy: intervals are water-saturated and have lost all aspects of original bedding.

The degree of fracturing in indurated sediments and in metamorphic and igneous rocks is described using the following categories:

1. Slightly fractured: core pieces are in place and contain little drilling slurry or breccia.
2. Moderately fragmented: core pieces are in place or partly displaced, but original orientation is preserved or recognizable (drilling slurry may surround fragments).
3. Highly fragmented: pieces are from the interval cored and probably are in the correct stratigraphic sequence (al-

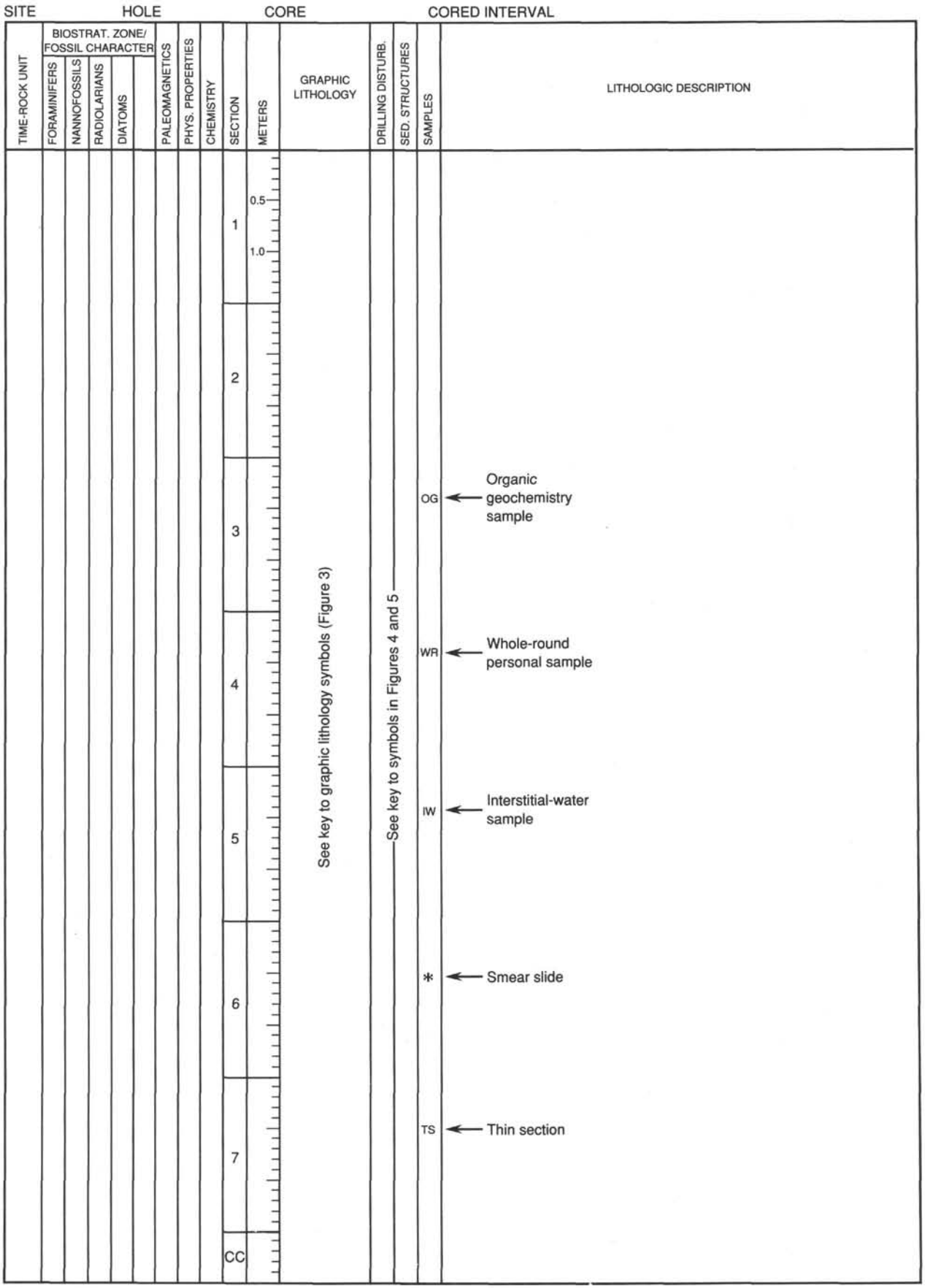

Figure 3. Visual core description forms used for sediments, sedimentary rocks, serpentine, and serpentinites.

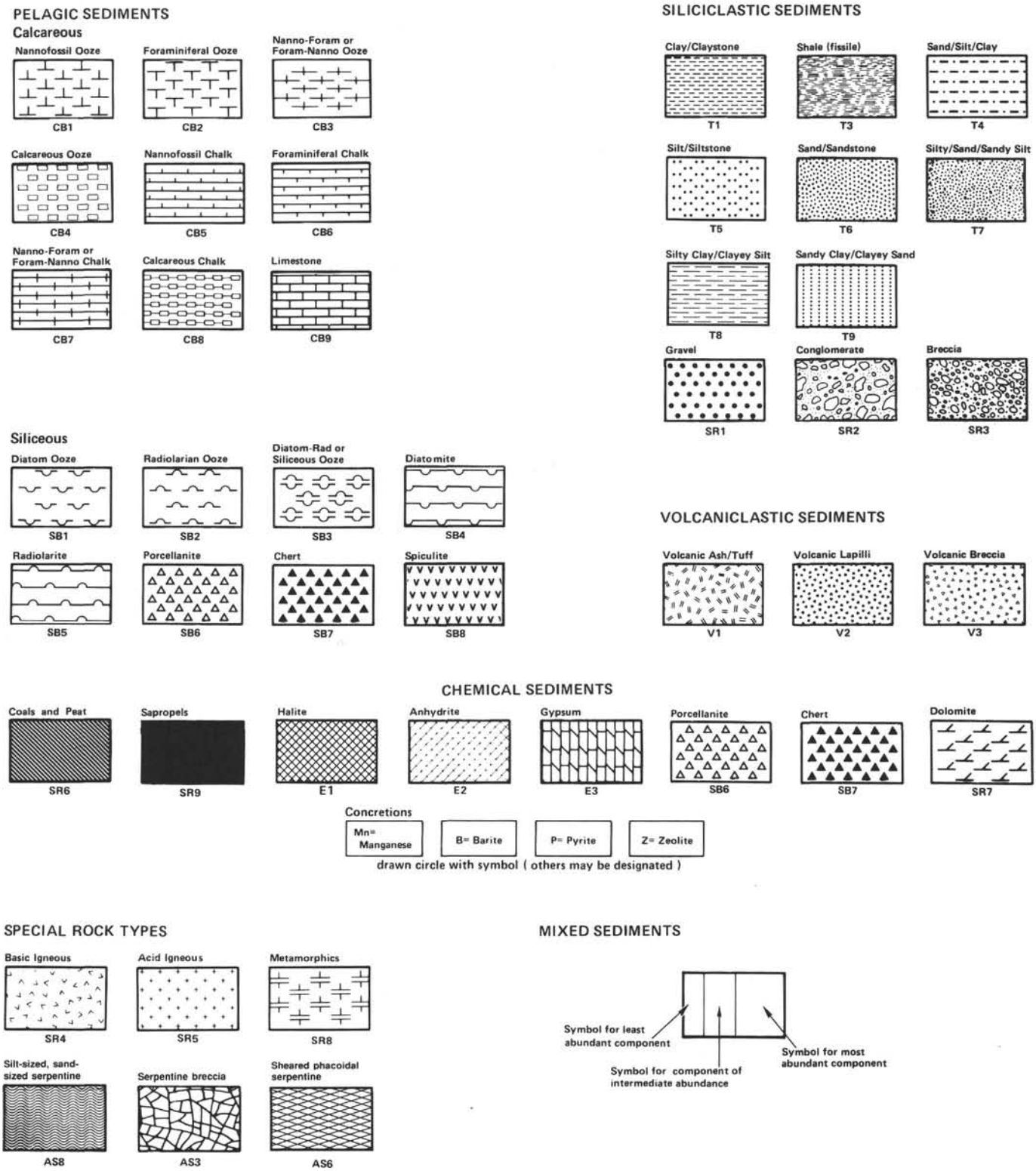

Figure 4. Key to symbols used in the "Graphic Lithology" column on the visual core description form shown in Figure 3.

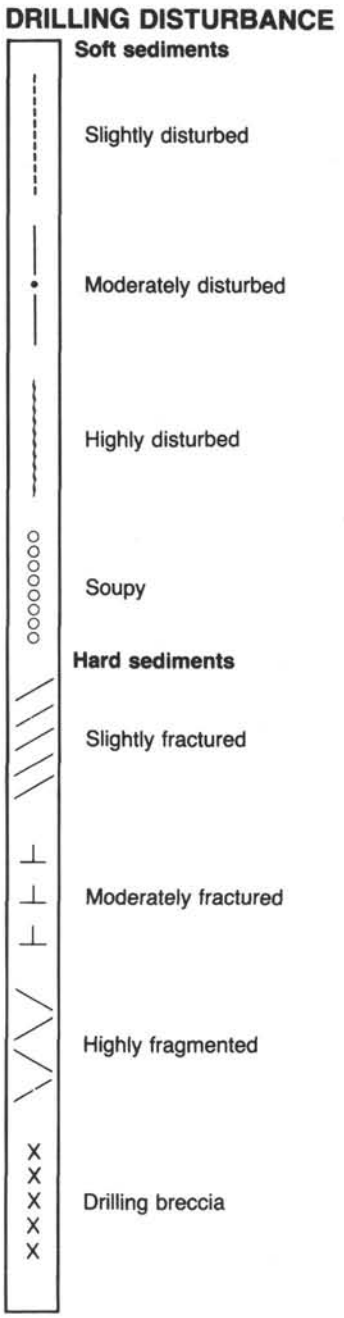

Figure 5. Symbols used for drilling disturbance.

though they may not represent the entire section), but their original orientation is completely lost.

4. Drilling breccia: core pieces have lost their original orientation and stratigraphic position and may be mixed with drilling slurry.

Sedimentary and Tectonic Structures

In sediment cores, natural structures and structures created by coring can be difficult to distinguish. Natural structures observed are indicated in the "Sedimentary Structure" column of the core description form. The symbols used to describe the primary structures (both biogenic and physical sedimentary structures) and secondary structures (including tectonic structures) are shown in Figure 6. A sedimentary structure observed frequently in sediments

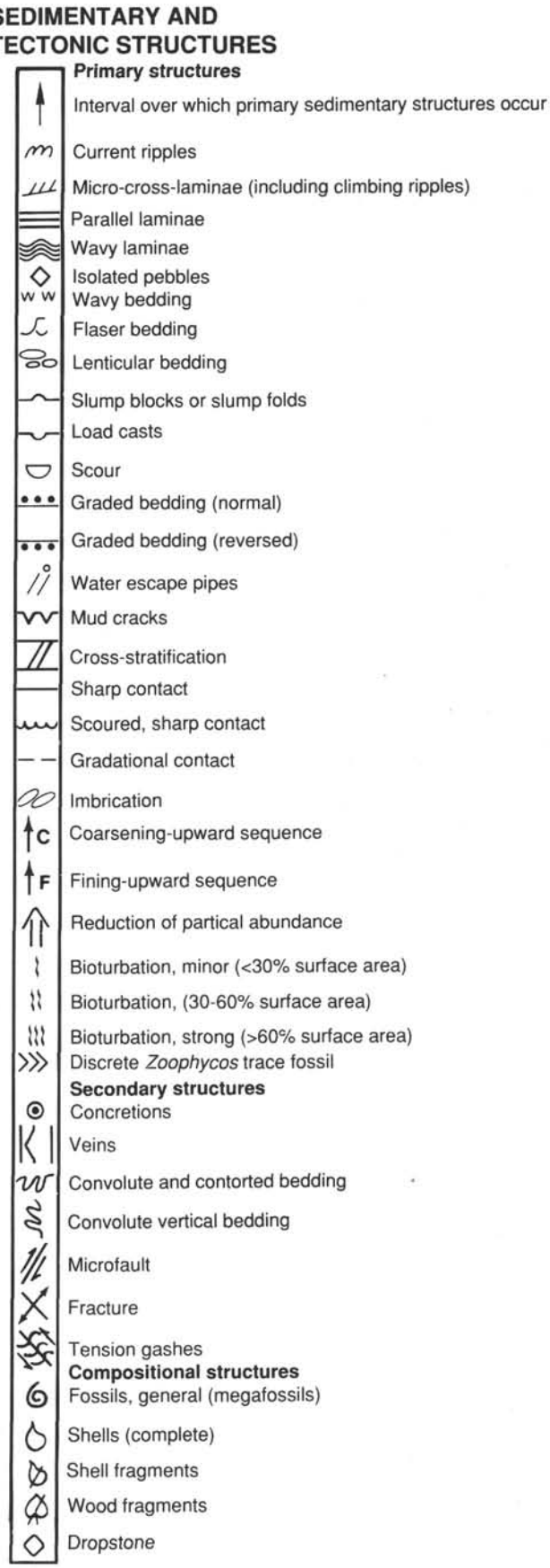

Figure 6. Symbols used for sedimentary and tectonic structures.

from Leg 125 is a decreasing concentration upward or downward of particles of approximately equal size. This structure is often observed overlying and underlying beds of vitric ash, where the ash concentration decreases upward within the background sediment. This structure has been interpreted as the result of animal activity that has redistributed ash into the sediment (Bramlette and Bradley, 1942); there is little evidence at Leg 125 sites for bottom-current activity. This structure is termed "fining-upward" or "coarsening-upward" (in deference to existing definitions) or reduction of particle abundance. Convolute vertical bedding is a secondary structure commonly observed in the serpentine units on these seamounts. This structure is commonly associated with foliation, which affects the hardness of clasts within the breccia and is related to post-depositional movement.

Color

Colors of the recovered material (sedimentary, metamorphic, and igneous) are determined by comparison with the Munsell soil-color charts. Colors are determined immediately after the cores have been split because chemical changes may occur when sediments are exposed to the atmosphere; consequently, some colors are ephemeral in deep-sea sediments (Moberly and Klein, 1976). Information on core colors is given in the text of the "Lithologic Description" column on the core description forms.

Samples

The position of samples taken from each core for shipboard analysis is indicated in the "Samples" column on the core description form. The symbol "*" indicates the location of samples used for smear-slide analysis. The symbols "TS," "XRD," and "XRF" indicate the location of samples for shipboard thin sections, XRD analysis, and XRF analysis, respectively. In some cases, an attempt was made to prepare a thin section from material unsuitable for that purpose. Although these sections exist in the thin-section collection at ODP, their poor quality did not permit us to make detailed descriptions. The locations of these samples are indicated by the symbol "X." The symbols "IW," "OG," "PP," and "WR" designate the location of samples for whole-round, interstitial-water geochemistry, frozen organic geochemistry, physical-properties, and personal samples, respectively.

Although not indicated in the "Samples" column, positions of samples for routine physical-properties (porosity [%], wet-bulk density [g/cm^3], and velocity [m/s]) and geochemical (% $CaCO_3$, % organic carbon [OC]) analyses are indicated by a dot and analytical results are presented in the "Physical Properties" column and in the "Chemistry" column. Paleomagnetic results (intervals of normal and reversed polarity) are indicated in the "Paleomagnetics" column. Intervals for which polarity could not be determined are indicated by a question mark.

Shipboard paleontologists generally base their age determinations on core-catcher samples, although additional samples from other parts of the core may be examined when required. Examination of such samples may lead to the recognition of zonal boundaries in the core; these are indicated in the appropriate column. All paleontological sample locations are shown, even if the samples are barren.

Lithologic Description - Text

The lithologic description that appears on each core description form consists of two parts: (1) a heading that lists all the sediment types (see "Classification of Sediment and Sedimentary Rock" section, this chapter) observed in the core, and (2) a more detailed description of these sediments, including data about color, location in the core, significant features, etc. In cases where there are thin beds of minor lithology, a description, including location information, is included in the text, but the beds may be too thin (cm) to appear in the graphic lithology column.

Smear Slide Summary

A table summarizing data from smear slides and thin sections (where available) appears on each core description form. The table includes information about the section and interval from which the sample was taken, whether the sample represents a dominant ("D") or a minor ("M") lithology in the core, and the percentages of sand, silt, and clay, together with all identified components (total 100%). As explained in the following section, these data are used to classify and name the recovered material.

CLASSIFICATION OF SEDIMENT AND SEDIMENTARY ROCK

The sediment classification scheme used during Leg 125 is similar to classification schemes used for previous DSDP and ODP legs. It is descriptive, using composition and texture as the only criteria to define sediment or sedimentary rocks. A primary sediment name is based upon, and named after, a component (or components) that constitutes 60% or more of the sediment. This classification scheme differs from some prior DSDP and ODP sediment classifications in the use of compositional modifiers.

Data for classifying sedimentary material come principally from shipboard visual analyses of smear slides using a petrographic microscope. These are qualitative optical estimates of particle characteristics (mineralogy, biogenic type, grain size, relative particle abundance, etc.) and differ from quantitative analyses of grain size, carbonate content, mineralogy, etc. Smear slide estimates of distinctive major components are accurate to within 5%, but estimates of minor constituents are accurate only to within 10%.

Composition and Texture

The Leg 125 sediment classification is descriptive, rather than genetic, and rock types are classified by their composition and texture. For example, the genetic terms pelagic, hemipelagic, turbidite, debris flow, etc., do not appear in this classification. The term "clay" is used for clay minerals and terrigenous material less than 4 mm in size without regard to origin. Biogenic components of silt or clay size are not described in textural terms. Thus, nannofossils present as silt-sized biogenic grains do not yield the sediment name of "nannofossil silt." Shipboard sedimentologists chose to use this classification (1) to maintain an internal consistency when naming intermediate mixtures of nonbiogenic and/or biogenic components and (2) to provide simple descriptive modifiers that indicate the important components and their abundance in the sediments.

Induration of Sediments

Determination of induration is subjective. For calcareous sediments and sedimentary rocks, three classes of induration or lithification have been recognized (Gealy et al., 1971):

1. Soft: sediment has little strength, is readily deformed under the pressure of a finger or the broad blade of a spatula, and is termed "ooze."

2. Firm: sediment is partially lithified, readily scratched with a fingernail or the edge of a spatula, and is termed "chalk."
3. Hard: sediment is well lithified and cemented, is resistant or impossible to scratch with a fingernail, and is termed "limestone" or "dolomite."

A continuum exists for siliceous biogenic sediments and sedimentary rocks between soft siliceous oozes, firm diatomites and radiolarites, and hard porcellanites and cherts. Two categories of induration have been recognized:

1. Soft: a sediment core may be split with wire cutter and is termed "ooze."
2. Hard: a core must be cut by a diamond saw, rather than a wire, and is called "porcellanite" or "chert."

Rules for Classification

1. About 60% of a component or group of components (e.g., total biogenic silica or biogenic carbonate) determines the principal name. The following main names are used:

Nonbiogenic: If the total of a nonbiogenic component, except serpentine and/or aragonite, is greater than 60%, the main name is determined by the dominant size(s) as defined in Shepard (1954; see Fig. 7), using the size classes defined by Wentworth (1922; see Fig. 8). Materials containing 60% or more of serpentine or aragonite are discussed in the section on "Serpentine and Serpentinite Classification" (this chapter). Examples of nonbiogenic principal names are clay, silt, silty clay, or sand. The terms sand-sized, silt-sized, etc., may be added to the name as a modifier.

Biogenic: If the total of biogenic components is greater than 60%, the principal name is "ooze," or the appropriate term denoting sediment induration (see the following).

2. A value of 30% to 60% of a component qualifies for major modifier status. The following terms are used as major modifiers:

Nonbiogenic: silty, clayey, sandy, etc., or a specific mineral composition (e.g., serpentine).

Biogenic carbonate: nannofossil, foraminifer, or calcareous (should be as specific as possible).

Biogenic silica: diatom, radiolarian, or siliceous biogenic (should be as specific as possible).

3. A value of 10% to 30% of a component qualifies for minor modifier status and is hyphenated with the word "rich" (e.g., nannofossil-rich clay, serpentine-rich clay).
4. A value of 5% to 10% of an unusual, important component (e.g., serpentine, zeolite, organic carbon, dolomite, thulite) also qualifies for minor modifier status, but is hyphenated with the word "bearing" (e.g., zeolite-bearing clay).
5. The most abundant component appears nearest the principal name. Major and minor modifiers are listed in order of decreasing abundance to the left of the principal name (e.g., foraminifer-rich nannofossil clay for a sediment containing 10% foraminifers, 30% nannofossils, and 60% clay).
6. Marl is defined as containing 30% to 60% $CaCO_3$, the remainder being mostly clay; thus, an ooze contains greater than 60% $CaCO_3$.
7. For nonbiogenic and calcareous sediments, the suffix "-stone" has been added to the main name if the core is sufficiently indurated that it had to be cut by the diamond saw.
8. For siliceous, indurated sediments, the term "porcellanite" describes a dull, brown to white, porous rock that contains clay, zeolites, or carbonate. Chert is denser and harder than porcellanite. These two siliceous rock types usually can be readily distinguished in hand specimen and are sufficient for shipboard descriptions.

VOLCANICLASTIC SEDIMENTS AND ROCKS

Because of difficulties in distinguishing volcanogenic sedimentation mechanisms (air fall, pyroclastic flow, debris flow, turbidity currents, etc.) in cores, the volcaniclastic classification scheme used during Leg 125 is primarily descriptive. Texture and composition are the only criteria used to define volcaniclastic sediments and rocks; the following scheme has been modified after schemes proposed and discussed by Schmid (1981), Fisher and Schmincke (1984), and others.

Textural terms used are those in common usage and are based upon grain size. For volcanic particles the terms "block," "lapilli," and "ash" are used; for nonvolcanic particles the standard Wentworth (1922) terminology is used (gravel, sand, silt, clay). The terms "breccia" and "conglomerate," denoting angular and rounded clasts, respectively, are applicable to both volcanic and nonvolcanic sediments and rocks. These textural names have been modified with compositional terms on the basis of composition of volcanic grains and clasts. For simplicity three major compositional terms are used: "vitric" for glass particles, "crystal" for mineral particles, and "lithic" for either volcanic or nonvolcanic rock fragments.

Note that this special terminology is applicable only to those sediments and sedimentary rocks where volcaniclastic detritus is present in amounts greater than 60%. Where this detritus occurs in amounts between 60% and 30%, the modifying term "volcanic" is applied. The classification format is given in Table 1.

Rules for Classification

1. Greater than 60% of the sediment or rock consists of volcaniclastic material.
2. A textural term and the state of lithification determine the primary name:

The term "block" is used for a particle size of 64 mm, both nonindurated and indurated sediments are termed "pyroclastic breccia," and the matrix composition is greater than or equal to 60% ash or lapilli.

The term "lapilli" is used for a particle size of 64 to 2 mm, "lapilli tephra" when nonindurated, and "lapilli tuff" when indurated.

The term "ash" refers to a particle size of mm, "vitric/crystal/lithic ash" when nonindurated, and "vitric/crystal/lithic tuff" when indurated.

3. A compositional term forms the major modifier. Multiple modifiers are employed in order of increasing abundance of admixed components, with the modifier nearest the principal term denoting the most abundant admixed component, preceded by modifiers denoting minor components using the terms "-bearing" and "-rich," following the rules previously outlined for sediments and sedimentary rocks. Three compositional terms are used:

"Vitric" refers to a glass particle (bubble-wall, pumiceous, etc.).

"Crystal" refers to a mineral particle (euhedral or anhedral).

"Lithic" refers to a rock fragment (volcanic or nonvolcanic).

SERPENTINE AND SERPENTINITE CLASSIFICATION

Serpentine deposits present a special problem in nomenclature. Textural and compositional criteria for Leg 125 deposits argue for emplacement as cold gravitational flows, either as low- or high-viscosity flows. Thus, these deposits are neither sediment nor igneous rock. Field geologists commonly describe this type of serpentine deposit as a "sedimentary serpentinite" (e.g., Cowan and Mansfield, 1970), but clearly this name is inappropriate for use with Leg 125 material. Use of such terminology could imply tranquil particle-by-particle deposition through the water column of particulate grains of serpentine. Leg 125 scientists therefore have chosen to establish a specific nomenclature and set of criteria applied to data collected from smear slides and the degree of induration of the core.

This classification includes poorly to lithified serpentine-rich materials with clastic, brecciated, or sheared phacoidal textures. Aragonite, chlorite, epidote, zoisite, etc., may be present in addition to serpentine as authigenic, primary or secondary minerals. Aragonite is commonly associated with serpentine in the Leg 125 material, with some occurrences in greater abundance than the serpentine. For material to be classified in this category, it must consist of 60% or more serpentine or nonbiogenic aragonite and contain less than 10% clay and/or biogenic components. If less than 10% clay and/or biogenic components are present, then the material may be primary (the product of igneous, alteration, or tectonic processes) or secondary (sedimentary or detrital) in origin. In situations of potentially equivocal origin, this Leg 125 classification scheme for serpentine deposits is descriptive, rather than genetic.

Rules for Classification

1. If serpentine or aragonite abundance is 60% or more in a nonindurated deposit, then the principal name is "serpentine" or "aragonite," respectively. The principal name is preceded by appropriate textural and compositional modifiers.

2. The textural modifier is classified nearest the principal name; it is based on the dominant sizes, as defined in Shepard (1954; see Fig. 7), and the size classes, as defined by Wentworth (1922; see Fig. 8). Examples are silt-sized serpentine and sand-sized serpentine.

3. The compositional modifiers are listed in order of decreasing abundance to the left of the textural modifier and the principal name.

A value of 30% to 60% of a component qualifies for major compositional modifier status. Example: chlorite sand-sized serpentine.

A value of 10% to 30% of a component qualifies for minor compositional modifier status and is hyphenated with the word "rich." Example: zoisite-rich sand-sized serpentine.

A value 5% to 10% of an unusual, important component (e.g., aragonite) qualifies for minor compositional modifier status and is hyphenated with the word "bearing." Example: aragonite-bearing zoisite-rich chlorite silt-sized serpentine.

4. A lithified or indurated form of serpentine is called serpentinite. The preceding definitions apply for textural and compositional modifiers.

5. If large clasts are set in a finer-grained serpentine matrix, then the material is named serpentinite breccia (without tectonic or sedimentary implications) with subsequent modifiers describing the matrix.

6. Sheared phacoidal serpentine is composed of scales or chips of serpentine from 1 mm to larger in size, which may have slickensided surfaces, and whose long axes define an anastomosing foliation. This foliation may enclose angular to subangular blocks of unsheared serpentinite (1 cm or larger in size) or may be associated with horizontal or vertical convolute bedding.

When serpentine is present in amounts of less than 60% or is not associated with nonbiogenic aragonite greater than 60%, the sediment and sedimentary-rock classification scheme previously described is used. The implication is that if more than 10% clay and/or biogenic components are present, then the material is probably deposited as a sediment.

Table 1. Classification of volcaniclastic sediments and rocks.

Clast size	Proportion of volcanic to nonvolcanic clasts 100%	60%	30%	0%
Block	Pyroclastic breccia	Vitric volcanic breccia or vitric volcanic conglomerate		Volcanic-rich or volcanic-bearing
Lapilli	Lapilli tephra	Vitric volcanic breccia or vitric volcanic conglomerate		Volcanic-rich or volcanic-bearing
	Lapilli tuff	Vitric volcanic breccia or vitric volcanic conglomerate		Volcanic-rich or volcanic-bearing
Ash	Vitric/crystal and/or lithic ash	Vitric volcanic sand/silt/clay		Volcanic-rich or volcanic-bearing
	Vitric/crystal and/or lithic tuff	Vitric volcanic sandstone, siltstone, claystone		Volcanic-rich or volcanic-bearing

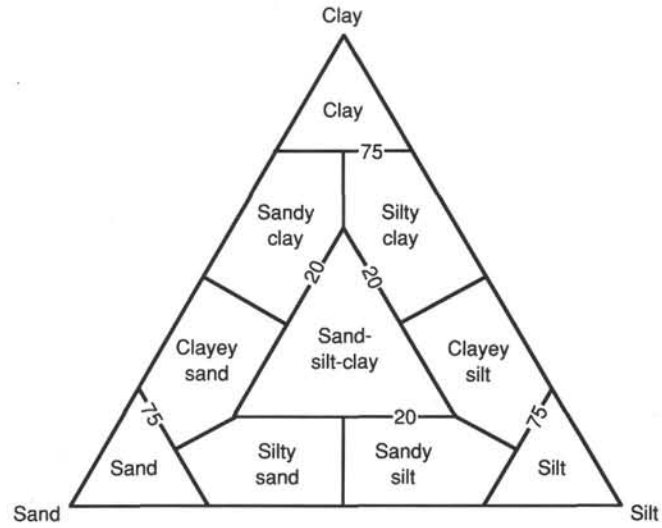

Figure 7. Sediment classification after Shepard (1954), with the sand-, silt-, and clay-sized fractions based on the Wentworth (1922) grain-size scale.

BIOSTRATIGRAPHY

General Remarks

The general correlation between biostratigraphic zones and the record of magnetic polarity reversals, seafloor magnetic anomalies, and an absolute time scale (Figs. 9 to 11) is based upon the scheme given by Berggren et al. (1985). Each

MILLIMETERS	μm	PHI (Ø)	WENTWORTH SIZE CLASS	
		-20		
4096		-12	Boulder (-8 to -12 Ø)	
1024		-10		
256		-8	Cobble (-6 to -8 Ø)	GRAVEL
64		-6		
16		-4	Pebble (-2 to -6 Ø)	
4		-2		
3.36		-1.75		
2.83		-1.5	Granule	
2.38		-1.25		
2.00		-1.0		
1.68		-0.75		
1.41		-0.5	Very coarse sand	
1.19		-0.25		
1.00		0.0		
0.84		0.25		
0.71		0.5	Coarse sand	
0.59		0.75		
1/2 — 0.50	500	1.0		
0.42	420	1.25		
0.35	350	1.5	Medium sand	SAND
0.30	300	1.75		
1/4 — 0.25	250	2.0		
0.210	210	2.25		
0.177	177	2.5	Fine sand	
0.149	149	2.75		
1/8 — 0.125	125	3.0		
0.105	105	3.25		
0.088	88	3.5	Very fine sand	
0.074	74	3.75		
1/16 — 0.0625	63	4.0		
0.053	53	4.25		
0.044	44	4.5	Coarse silt	
0.037	37	4.75		
1/32 — 0.031	31	5.0		
1/64 0.0156	15.6	6.0	Medium silt	
1/128 0.0078	7.8	7.0	Fine silt	
1/256 — 0.0039	3.9	8.0	Very fine silt	MUD
0.0020	2.0	9.0		
0.00098	0.98	10.0	Clay	
0.00049	0.49	11.0		
0.00024	0.24	12.0		
0.00012	0.12	13.0		
0.00006	0.06	14.0		

Figure 8. Wentworth (1922) grain-size scale.

microfossil zonation is then fitted into this reversal/anomaly scheme for the Quaternary to middle Eocene. Some minor differences between the scheme of Berggren et al. (1985) and that used for Leg 125 are discussed in the individual sections for each fossil group.

Age assignments are based mainly on core-catcher samples. Additional samples were studied when the core-catcher samples were found barren or restricted to narrow time intervals or when boundaries or unconformities occurred. Sample locations, preservation, and abundance for each fossil group are indicated on the barrel sheets.

Calcareous Nannofossils

The standard calcareous nannoplankton zonation (Martini, 1971; Bukry, 1973; Okada and Bukry, 1980; Backman, Duncan, et al., 1988) is used at all sites to identify the nannoplankton zones. The Pliocene/Pleistocene boundary is defined by the first occurrence of *Gephyrocapsa oceanica*, at the top CN13 Zone of Okada and Bukry (1980). The Miocene/Pliocene boundary is defined by the last occurrence of *Triquetrorhabdulus rugosus* or the last occurrence of *Discoaster quinqueramus* (within CN10a Subzone). The Oligocene/Miocene boundary is defined by the last occurrence of *Sphenolithus ciperoensis* and *Dictyococcites bisectus* (at top of CP19b Subzone or NP25 Zone). The Eocene/Oligocene boundary corresponds to the last appearance of *Discoaster barbadiensis* or *Discoaster saipanensis* (at the top of NP20 Zone or CP15b Subzone).

Nannofossil Abundance and Preservation

Calcareous nannofossils were examined in smear slides prepared from sediment. The abundance of nannofossils is estimated as follows:

A = abundant (10 specimens/field of view).
C = common (1–10 specimens/field of view).
F = few (1 specimen/2–10 fields of view).
R = rare (1 specimen/100 fields of view).

The state of preservation is estimated as follows:

G = good (no or only minor signs of dissolution or overgrowth of placoliths and discoasters).

M = moderate (slight to moderate dissolution of placoliths, discoasters, and others or slight to moderate overgrowth especially on discoasters and other ortholithic forms).

P = poor (severe dissolution in placoliths with abundant broken specimens or heavy overgrowth of discoasters and sphenoliths).

Planktonic Foraminifers

Neogene

The zonation of Blow (1969), as amended by Kennett and Srinivasan (1983), is followed in this volume. This zonation is based on a phylogenetic lineage, using species ranges compiled from Kennett and Srinivasan (1983). The first appearance of *Globorotalia truncatulinoides*, between Zones N21 and N22, marks the Pliocene/Pleistocene boundary. The Miocene/Pliocene boundary, between Zones N18 and N19, is based on the first appearance of *Sphaeroidinella dehiscens*, and the Oligocene/Miocene boundary is equated with the first appearance of *Globoquadrina dehiscens*. The unamended zonation of Blow (1969) for the Neogene was used in this part of the northern Pacific during DSDP Legs 6, 55, 59 and 60.

Paleogene

The tropical zonation of Blow (1969, 1979) is applied to the upper Eocene–Oligocene section, and Berggren's (1977) zonation is used for the Paleocene–middle Eocene.

Methodology

All samples are disaggregated in a hot detergent solution, with Calgon added to clayey samples, and washed over a 63-mm sieve. The following categories describe the frequencies of planktonic foraminifers in each sample, relative to other sand-sized particles:

A = abundant (25% of the residue).
C = common (1–25% of the residue).
F = few (1–5% of the residue).
R = rare (% of the residue).
B = barren (no foraminifers, or rare benthic foraminifers only).

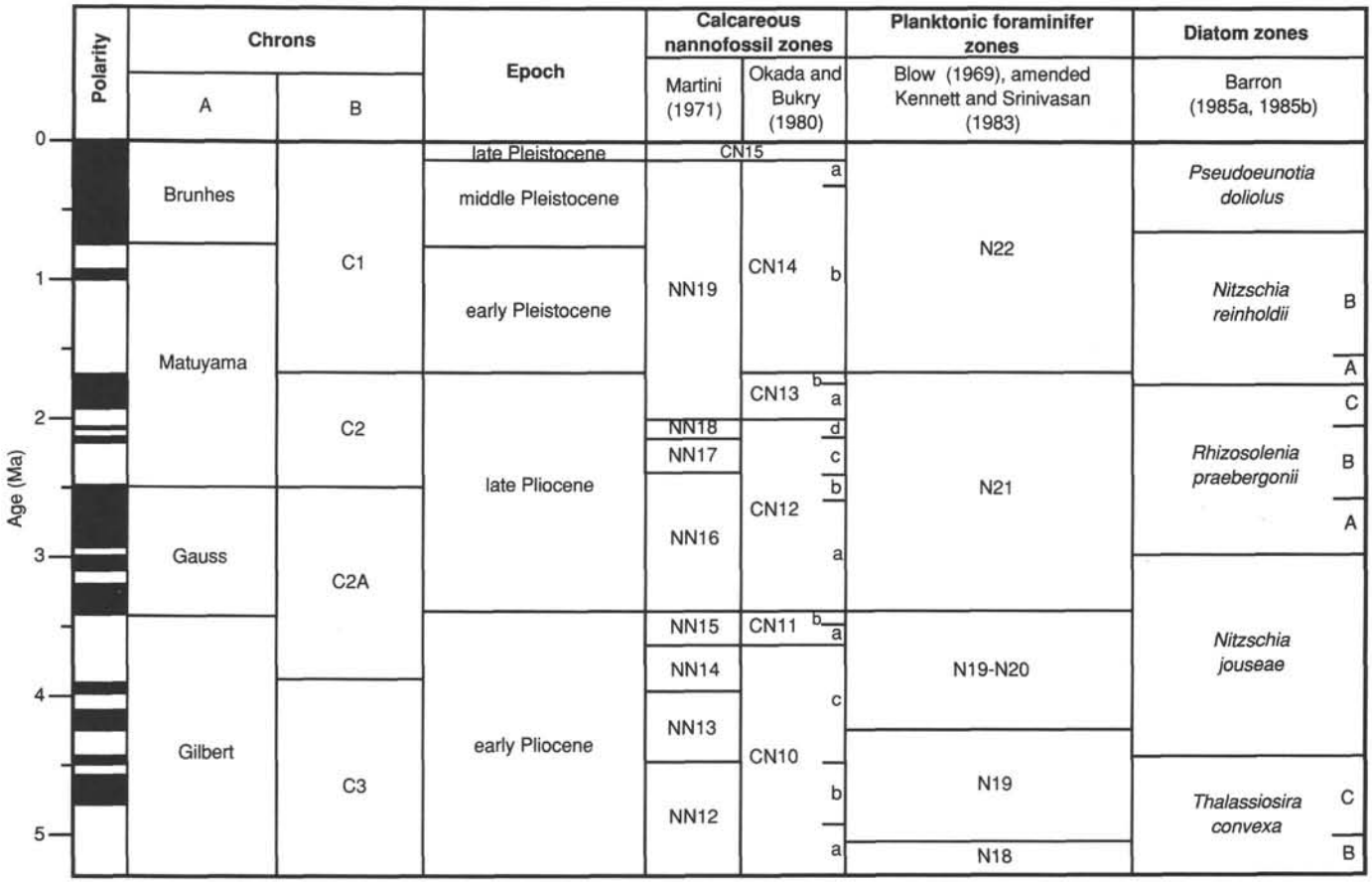

Figure 9. Correlation of Pleistocene to Pliocene chronostratigraphy, biostratigraphy, and magnetostratigraphy used during Leg 125.

The preservation of foraminifers is described as follows:

G = good (little or no fragmentation and/or recrystallization).
M = moderate (some signs of dissolution (fragmentation and dissolution holes) and/or some recrystallization);
P = poor (severe dissolution and/or recrystallization).
B = barren (lacks planktonic foraminifers or undiagnostic juveniles associated with benthic foraminifers).

Diatoms

The Oligocene through Holocene diatom zonation proposed by Barron (1985a, 1985b) for the equatorial Pacific is used during Leg 125. Koizumi (1986) showed that Barron's equatorial Pacific zonation is applicable for both the Mariana and Izu-Bonin areas. This zonation consists of 20 zones and 23 subzones and is based on Burckle's (1972) late Miocene through Quaternary zonation and Barron's (1983) late Oligocene to middle Miocene zonation. Although the chronostratigraphy used during Leg 125 follows Berggren et al. (1985), this time scale does not incorporate a diatom zonation. Therefore, correlations follow those of Barron (1985a, 1985b). Significant contributions to the understanding of the Neogene diatom biostratigraphy from this region include studies by Burckle (1972, 1977, 1978) and Burckle and Trainer (1979), as summarized and modified by Barron (1985a, 1985b).

Shipboard samples are prepared by the following standard procedure: (1) 1 cm^3 of sediment is placed in a 250-mL beaker, (2) 10% HCl is added until the carbonate reaction ceases, (3) the sample is heated in 10% H_2O_2, and then (4) washed repeatedly in distilled water. Strewn slides of cleaned material are prepared using a Hyrax mounting medium, and identifications are made at magnifications of 1000×. Diatom abundance is determined at 400× magnification, according to the following comparison:

A = abundant (50 diatoms/transect).
C = common (10–50 diatoms/transect).
F = few (1–10 diatoms/transect).
R = rare (1–32 diatoms/slide).
T = trace (only rare fragments of diatoms).
B = barren (no fragments identifiable as diatom remains seen).

Estimates of preservation for shipboard analysis can only be approximate and subjective. A more precise and objective classification might be achieved during shorebased laboratory studies.

SEDIMENT/FLUID GEOCHEMISTRY

Sediment Geochemistry

Sediments are analyzed on board ship for inorganic carbon and for total nitrogen, carbon, and sulfur. The organic carbon content of the sediments is then calculated by difference. Inorganic carbon content is determined for all sediment samples taken for physical-properties measurements and for additional samples as necessary, at a frequency of about one per section. Total nitrogen, carbon, and sulfur are determined for a subset of these samples, at a frequency of about one per core. All samples are freeze-dried prior to analysis.

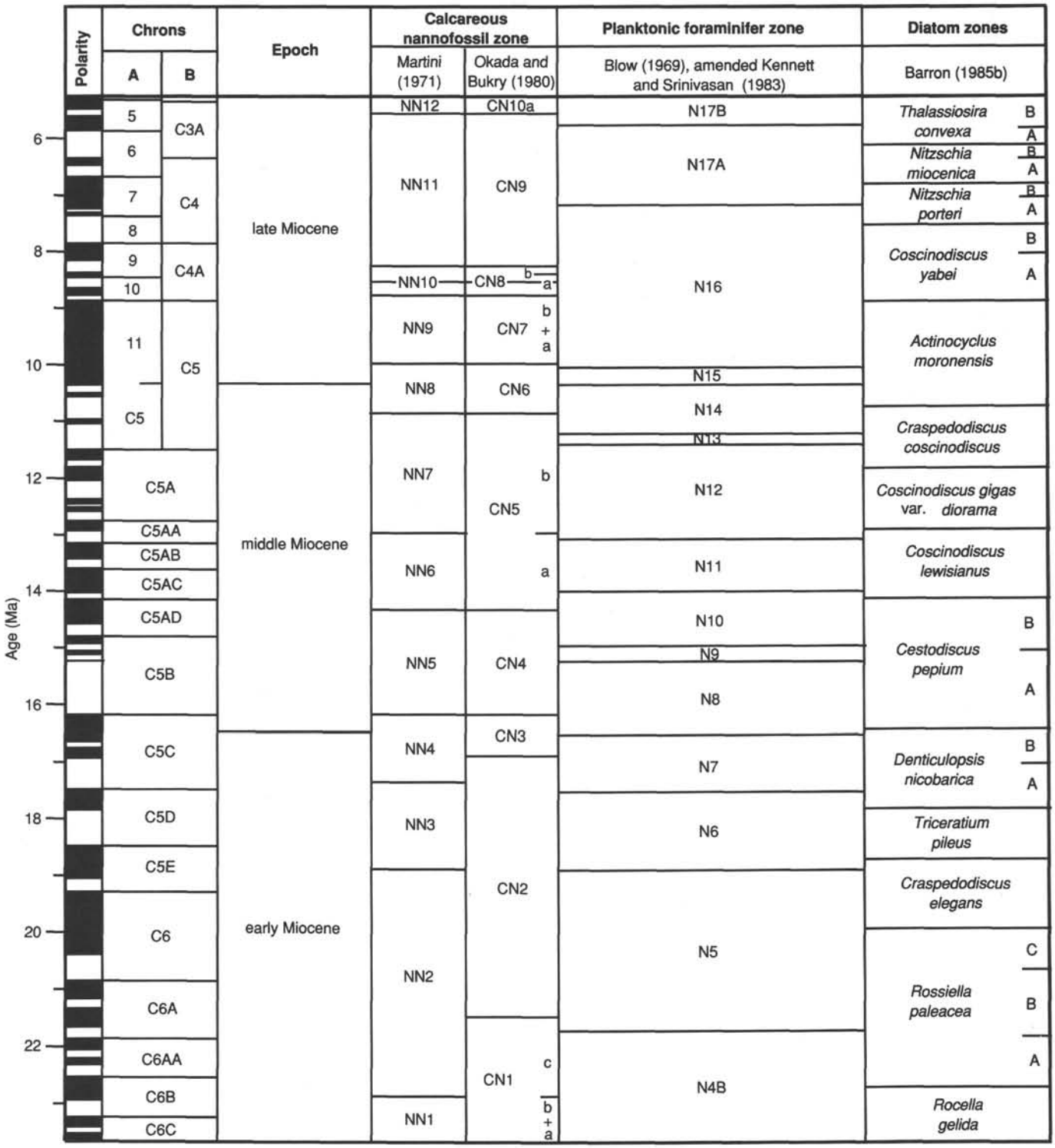

Figure 10. Correlation of Miocene chronostratigraphy, biostratigraphy, and magnetostratigraphy used during Leg 125.

Total inorganic carbon is determined using a Coulometrics 5011 coulometer equipped with a System 140 carbonate carbon analyzer. Depending on carbonate content, 15 to 70 mg of ground and weighed sediment is reacted in a 2N HCl solution. The liberated CO_2 is titrated in a monoethanolamine solution with a colorimetric indicator, while monitoring the change in light transmittance with a photodetection cell.

Total nitrogen, carbon, and sulfur are determined using an N/C/S analyzer, model NA 1500 from Carlo Erba Instruments. Bulk samples are combusted at 1000°C in an oxygen atmosphere, converting organic and inorganic carbon to CO_2 and sulfur to SO_2. These gases, along with nitrogen, are then separated by gas chromatography and measured using a thermal-conductivity detector.

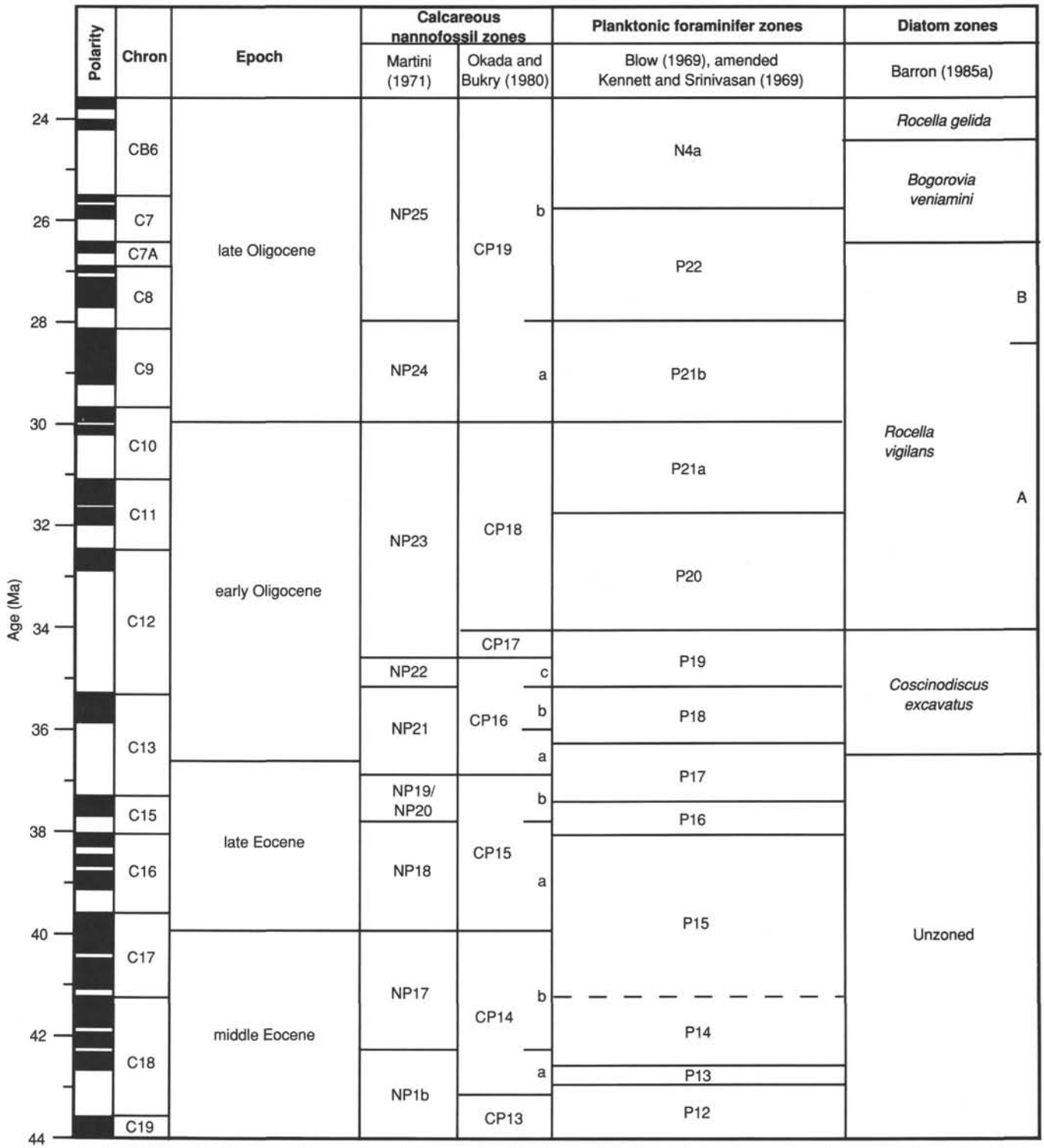

Figure 11. Correlation of Oligocene to late Eocene chronostratigraphy, biostratigraphy, and magnetostratigraphy used during Leg 125.

Fluid Geochemistry

Hydrocarbon Gases

As required by safety considerations, the concentrations of the hydrocarbons methane (C_1), ethane (C_2), and propane (C_3) are monitored in the sediment cores at intervals of about 10 m. Hydrocarbon gases are extracted from bulk sediment using a headspace-sampling technique. As soon as the core arrives on deck, a 5-cm^3 plug of sediment is taken, using a No. 4 cork borer. This sample is placed immediately in a glass vial that is sealed with a septum and metal crimp and then heated to 70°C. The gas driven off is drawn into a syringe and injected into a Hach-Carle AGC Series 100 Model 211 gas chromatograph equipped with a thermal-conductivity detector. Where high concentrations of propane are suspected, a second sample is taken by the same method and analyzed for C_1 through C_6 hydrocarbons using a Hewlett-Packard 5980A

natural gas analyzer, a gas chromatograph equipped with Poropak-Q, molecular-sieve, and silicone-oil-coated columns, and a flame ionization detector. After the headspace gas is analyzed, the actual volume of the sediment sample is measured to the nearest 0.5 cm^3 by displacement using water. Details of this method and the complete configuration of both gas chromatographs are given in the "Explanatory Notes" chapter for Leg 112 (Shipboard Scientific Party, 1988).

Also analyzed using the Hach-Carle gas chromatograph are samples of suspected gas pockets in the cores. These samples are taken immediately upon recovery of the core by penetrating the transparent plastic core liner with a hollow stainless-steel punch equipped with a valve and hypodermic needle. The gases are collected through a rubber septum into an evacuated glass tube.

Interstitial Water

During Leg 125, interstitial water was obtained from sediments and unconsolidated serpentine by squeezing and by *in-situ* extraction using the Barnes pore-water sampler.

Whole-round sections of core 5 to 15 cm in length are squeezed. As soon as the core arrives on deck, these samples are cut by slicing the plastic core tube and capping both ends. The samples are then cooled to the appropriate *in-situ* temperature; removed from the core liner; scraped with a stainless-steel spatula to remove the outer, contaminated layer; and placed in a stainless-steel squeezer (Manheim and Sayles, 1974). Both the squeezer and the samples are handled only with plastic gloves to avoid contamination. The squeezer is placed in a Carver hydraulic press and squeezed at pressures of up to 40,000 psi. Interstitial water is collected directly into a 50-mL plastic syringe, from which the various aliquots for analysis are ejected through an on-line 0.45-mm polysulfone filter mounted in a Gelman "acrodisc" disposable filter holder. Squeezed interstitial waters here are designated "IW" samples.

The *in-situ* water sampler-temperature-pressure (WSTP) tool designed by R. Barnes was first used during Leg 110 (Barnes, 1988). This tool collects interstitial water while simultaneously measuring sediment temperature and pore pressure. The tool is lowered on the sand line to the end of the drill string, where it locks into an assembly just above the bit. The hole is flushed with drilling fluid with the bit just off bottom during the descent of the sampler to keep the hole free of fill. After the sampler is latched into place, the bit is lowered into the bottom with the sampling probe projecting about 20 cm through the bit. A timer-operated valve opens, and interstitial water is drawn under negative pressure through two 40-mm stainless-steel filters and one 1-mm polyester filter into the sampler. There it passes through a stainless-steel entry tube of 12-mL volume into two sample coils arranged in series and separated by an open ball valve, and then into a steel overflow cylinder of 1200 mL volume that also contains the sample coils and valves. This overflow cylinder generates negative pressure when the sampling valve is opened, as this cylinder is normally filled with air when the tool is sent downhole. For Leg 125, we evacuated this cylinder prior to deployment to prevent oxidation of H_2S in the sampler.

The tubing and coils are initially filled with distilled water, which is displaced into the overflow cylinder on sampling, along with any excess sample and about 1 mL of seawater from the dead volume outside the entry valve. The first of the two sample coils in series is made of stainless steel, has a volume of about 20 mL, and is used for the shipboard analyses. The second is copper, has a volume of 40 to 50 mL, and is typically used for shorebased determination of helium isotopes and dissolved gases. We also analyze the water from the overflow cylinder, as it often is useful for determining major and minor dissolved species. In particular, it sometimes shows higher calcium-to-chlorinity ratios than the undiluted sample from the steel coil, indicating that calcium carbonate has probably precipitated in the latter. The amount of dilution of the overflow aliquot can usually be determined from its chlorinity relative to that of the undiluted sample. The length of time required to fill the Barnes sampler varies with the permeability of the sediment, but typically is about 15 min. Interstitial-water samples collected with the Barnes tool are here designated "BW." When removed from the stainless-steel coil, they are filtered (0.45 mm) like the squeezed samples.

The waters are analyzed immediately when recovered for pH, alkalinity by potentiometric titration, salinity by refractive index, and (when an odor is detected) hydrogen sulfide by colorimetry using methylene blue. Aliquots are refrigerated and analyzed within a few days of collection for calcium, magnesium, and chlorinity by colorimetric titration; sulfate by ion chromatography; silica, ammonium, phosphate, and bromide by colorimetry; and potassium by flame atomic absorption spectrophotometry. All shipboard analyses are performed using standard ODP techniques, as detailed by Gieskes and Peretsman (1986) and described briefly in the "Explanatory Notes" chapter for Leg 112 (Shipboard Scientific Party, 1988). IAPSO standard seawater is the primary standard for determination of calcium, magnesium, and chlorinity and also provides a check on the accuracy of the analyses for alkalinity, potassium, sulfate, and bromide.

PALEOMAGNETISM

Paleomagnetic studies performed on board *JOIDES Resolution* include measurements of the remanent magnetization and magnetic susceptibility of sedimentary, igneous, and metamorphic material. Measurement of remanence is accompanied by alternating field (AF) demagnetization whenever possible in the hope of removing secondary magnetizations.

Instruments

A Molspin spinner magnetometer and a 2-G Enterprises pass-through cryogenic superconducting rock magnetometer are available for measuring remanence. An AF demagnetizer (Model 2G600) capable of alternating fields up to 25 mT is on-line with a cryogenic magnetometer. Both are controlled by a FASTCOM4 multiserial communication board in an IBM PC-AT compatible computer. For measuring the archive half of a core, Leg 125 scientists used a BASIC program (COREMAG), modified by C. Helsley from the SUPERMAG program used during Leg 124E. Up to seven discrete samples (individual samples taken from the working half of the core) can be measured on the cryogenic magnetometer in a single run using the program 7CUBE, modified by C. Helsley during Leg 124E from the SUPRCUBE program. The spinner magnetometer is controlled by a Digital PRO350 computer and is used only to measure discrete samples.

The superconducting quantum interference device (SQUID) sensors in the cryogenic magnetometer measure magnetization over an interval approximately 20 cm long. Each axis has a different response curve. The widths of the sensor regions imply that as much as 150 cm^3 of core contributes to the sensor signals, thereby blurring sharp magnetic transitions. The increased volume of rock within the sensor region permits one to determine accurately the remanence of weakly magnetized samples despite the relatively high back-

ground noise caused by the motion of the ship. The SQUID electronics operate at a 1× scale and use the flux-counting mode for most measurements.

Remanent Magnetization Measurements

The maximum AF demagnetizing field allowed for sections from the archive half is 15 mT or the median destructive field, whichever is lower. Discrete samples from the working half of the core also are demagnetized using the Schonstedt GSD-1 AF demagnetizer and thermal demagnetizer, although these samples are then exposed to ambient magnetic fields after demagnetization, but prior to measurement. Therefore, progressive AF and thermal demagnetizations of samples from Leg 125 and their measurement by cryogenic magnetometers will be performed in magnetically shielded laboratories on shore.

Sediments

Remanence measurements of sediments are performed by passing archive-half core sections of the APC cores through the cryogenic magnetometer. Measurements are taken at 10-cm intervals at both natural remanent magnetization (NRM) and the various AF demagnetization levels. These measurements contain the averaging effect of the responses of the three axes because of the broad sensor region in the cryogenic magnetometer; thus, deconvolution will be required to recover the higher frequency changes of magnetization.

Discrete samples are taken from APC, XCB, and RCB sediment cores. The sampling is performed by pressing a plastic box (6 cm^3) into the sediments and removing it. The uphole direction is marked on the box. For more consolidated sediments, a spatula is used to cut the cubes. At least one sample per section is taken in APC, XCB, and RCB cores. The sampling positions in XCB and RCB cores are unevenly controlled, mainly by the distribution of undisturbed portions of the core sections. More than one-third of the discrete samples were measured in the cryogenic magnetometer during Leg 125 after AF demagnetization to 2, 5, 10, and 15 mT.

Igneous and Metamorphic Rocks

To measure the remanence of igneous and metamorphic rocks, minicores of 1-in. diameter are taken where appropriate and measured in the cryogenic magnetometer. The NRM and AF demagnetization steps of archive-half sections containing pieces of core greater than 20 cm are measured in the cryogenic magnetometer at 3-cm intervals.

Magnetic Susceptibility Measurement

Magnetic susceptibilities are measured on all sediment and most igneous and metamorphic cores using a Bartington Instrument magnetic susceptibility meter (model M.S.1) with a M.S.1/CX 80-mm whole-core sensor loop set at 0.47 kHz. The susceptibility meter is on-line with the GRAPE and the *P*-wave logger on the multisensor track. Leg 125 scientists are the first to measure susceptibility with this configuration. The susceptibility of most material encountered during Leg 125 is high, and therefore all measurements are performed in the low-sensitivity mode. As susceptibility is a volume-dependent property, susceptibility data from incomplete cores are rejected.

In addition to characterizing the cored sediments, susceptibility data are used to correlate between holes and sites. Correlation of susceptibility data is performed by observing peak-to-peak spacings and general trends in the susceptibility curve. Absolute individual peak heights are not useful for correlation of susceptibility data.

IGNEOUS AND METAMORPHIC PETROLOGY

Core Curation and Shipboard Sampling

As standard procedure, igneous and metamorphic rocks recovered during coring are examined by petrologists to determine where the core should be split to best preserve unique features and/or to expose important structures. The core is split into archive and working halves using a rock saw equipped with a diamond blade. Care is always taken to ensure that orientation is preserved during splitting and prior to labeling, usually by marking the original base of each piece with red crayon. Each piece is numbered sequentially from the top of each section. Pieces are labeled at the top, uncut surface. Pieces that can be fitted together (reassembled like a jigsaw puzzle) are assigned the same number, but are lettered consecutively (e.g., 1A, 1B, 1C, etc.). Plastic spacers are placed between pieces having different numbers, but not between those having different letters and the same number. The presence of a spacer may represent a substantial interval of no recovery (or may not). If the original unsplit piece is long enough, such that the top and bottom can be distinguished before removal from the core liner (i.e., the piece could not have rotated top to bottom about a horizontal axis in the liner during drilling), an arrow is added to the label pointing to the top of the section. Because pieces are free to turn about a vertical axis during drilling, azimuthal orientation is not possible.

After the core is split, the working half is sampled for measurement of physical and magnetic properties and for XRF, XRD, and thin-section studies. These samples may take the form of minicores and, if appropriate, are stored in seawater prior to measurement. When recovery permits, samples are taken from each lithologic unit. The archive half is described on the visual core description (VCD) form, used for nondestructive physical-properties measurements (such as magnetic susceptibility), and photographed before storage.

Visual Core Descriptions

Igneous VCD forms are used when describing the basement cores (Fig. 12). The left column of the form is a graphic representation of the archive half. A horizontal line across the entire width of the column denotes a plastic spacer glued between rock pieces inside the liner. Oriented pieces are indicated on the form by an upward-pointing arrow to the right of the piece. Shipboard samples and studies are indicated on the VCD in the column headed "Shipboard Studies" using the following notation: XRD = X-ray-diffraction analysis; XRF = X-ray-fluorescence analysis; TS = petrographic thin section; PP = physical-properties analysis. In some cases, we attempted to prepare a thin section from material unsuitable for that purpose. Although these sections exist in the thin-section collection at ODP, their poor quality does not permit us to make a detailed description. These sections are indicated by the symbol "X."

Because igneous and metamorphic rocks are classified mainly on the basis of macroscopic mineralogy and texture, shipboard petrologists follow a checklist of features to ensure consistent and complete descriptions. To this end, VCDs are entered directly into a computerized data base (HARVI). This is advantageous because the HARVI program prompts the describer with a set of questions pertaining to petrologic features, all of which must be diagnosed and entered in the data base. The descriptions on the VCD forms will, to a certain extent, reflect the rigidity of the HARVI program. It is therefore relevant to discuss briefly the organization of the data base. Fine-grained rocks are entered into a data set called HARVI-F, and coarse-grained rocks are entered into the data

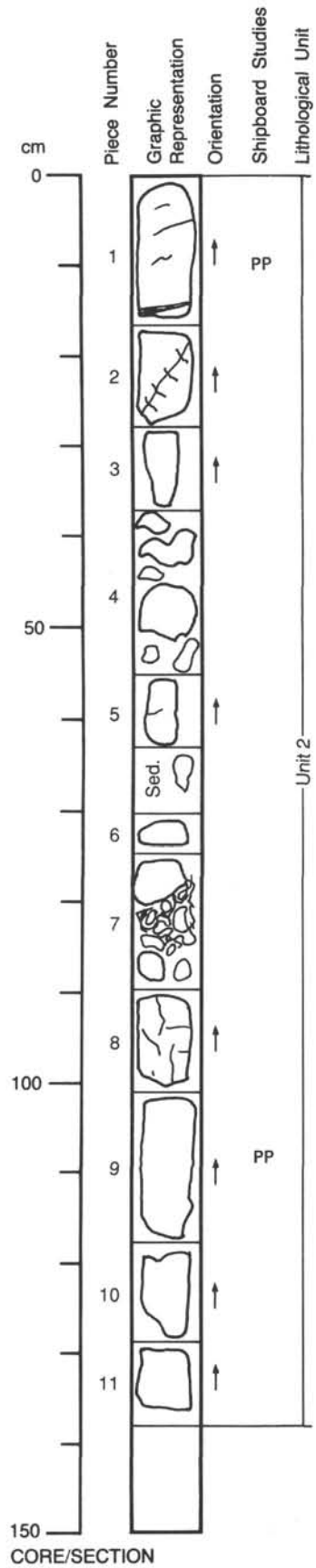

125-779A-35R-1

UNIT 2: TECTONIZED SERPENTINIZED HARZBURGITE

Pieces 1-3

COLOR: Bluish gray (5B 5/1).
LAYERING: Possible alignment of elongate orthopyroxene.
DEFORMATION: Elongate spinels in trains; wavy cleavage on orthopyroxene.
PRIMARY MINERALOGY:

Orthopyroxene - Mode: 15-25%.
Crystal size: 3-5 mm.
Crystal shape: Elongate-ragged.
Crystal orientation: Not visible.
Percent replacement: Variable.

Olivine - Mode: 75-85%.
Crystal size: 3-7 mm.
Crystal shape: Elongate-ragged.
Crystal orientation: Not visible.
Percent replacement: Variable.

Spinel - Mode: Trace.
Crystal size: <2 mm.
Crystal shape: Elongate-ragged.
Crystal orientation: Not visible.
Percent replacement: Variable.

SECONDARY MINERALOGY:

Serpentine.
Total percent: 40-80%.
Texture: N/A.
Vein material: Dark black amorphous serpentine-filled vein, <3 mm wide oriented almost parallel to core in Piece 2. This vein has <1-mm-wide and 2-cm-long white-green serpentine veins running perpendicular to it. Piece 1 has white-green serpentine vein, <2 mm wide, perpendicular to core.

UNIT 2: SERPENTINIZED HARZBURGITE

Pieces 4-8

COLOR: Dark greenish gray (5B 4/1).
LAYERING: None.
DEFORMATION: Piece 8 appears to be slightly tectonized and exhibits elongation of the pyroxene crystals.
PRIMARY MINERALOGY:

Olivine - Mode: 70-75%
Crystal size: 1-2 mm.
Crystal shape: Equant-elongate.
Crystal orientation: N/A.
Percent replacement: N/A.

Orthopyroxene - Mode: 25-30%.
Crystal size: 1-3 mm.
Crystal shape: Equant-elongate.
Crystal orientation: N/A.
Percent replacement: N/A.

Spinel - Mode: Trace.
Crystal size: <1 mm.
Crystal shape: Equant.
Crystal orientation: N/A.
Percent replacement: N/A.

SECONDARY MINERALOGY:

Serpentine.
Total percent: 70?
Texture: Serpentinized.
Vein material: <2-mm wide white-pale green serpentine (chrysotile?) veining; Piece 4 is mixed with serpentine sediment.

Figure 12. Visual core description form used for metamorphic and igneous rocks.

set HARVI-C. Each record is checked by the data-base program for consistency, and a hard copy is printed in a format that resembles the final barrel sheets. This copy is pasted directly onto a copy of the barrel sheet.

When describing sequences of fine- to coarse-grained rocks, the core is subdivided into lithologic units on the basis of changes in petrographic and rock-clast types and mineral abundances. For each lithologic unit, section, and rock type, the following information is recorded as appropriate using the HARVI system:

1. Leg, site, hole, core number, core type, and section.
2. Unit number (consecutive downhole), position in the section, number of pieces of the same lithologic type being described, the name of the describer, and rock name.
3. Color of the rock (recorded when the rock piece was dry) using the Munsell (1975) chart, presence of layering and deformation and character thereof. In the case of variably serpentinized ultramafic rocks, particular attention is paid to the presence of deformed cleavage surfaces of relict orthopyroxene ("bastite"), elongate spinel and olivine, and mylonitization and shearing as indicators of deformation.
4. The number of mineral phases and their distribution within the unit. For each mineral phase we note the following: (a) abundance (%), (b) average size in mm, (c) shape, (d) the degree of alteration, and (c) further comments. In the case of heavily serpentinized materials, the original grain size and shape of the primary phases may not be visible or are only estimated.
5. Groundmass texture: glassy, microcrystalline, fine-grained (<1 mm), medium-grained (1–5 mm), or coarse-grained (5 mm); relative changes of grain size within the unit (e.g., coarsening from Piece 1 to Piece 5).
6. Presence of alteration and alteration characteristics, including structures imposed during formation of secondary minerals, type of alteration, and abundance of secondary minerals.
7. Vesicles: percentage abundance, distribution, size, shape, and fillings and their relationships (including proportion of vesicles that are filled by alteration minerals).
8. Structure: massive flow, pillow lava, thin flow, breccia, hyaloclastite, etc., and comments.
9. Alteration: fresh (% alteration.), slightly (2%–10% alteration), moderately (10–40% alteration), highly (40%–80% alteration), very highly (80%–95% alteration), or completely (95%–100% alteration) altered; type, form, and distribution of alteration.
10. Veins/Fractures: percentage present, width, orientation, and fillings and their relationships. The relationship of the veins and fractures to the alteration is also noted.
11. Comments: notes on the continuity of the unit within the core, and the interrelationship of units are added here, when appropriate.

Basalts are termed aphyric (%), sparsely phyric (1%–2%), moderately phyric (2%–10%), or highly phyric (10%), depending upon the proportion of phenocrysts visible with the hand lens or binocular microscope (approximately 10×). Basalts are further classified by phenocryst type (e.g., a moderately plagioclase-olivine phyric basalt contains 2%–10% phenocrysts, mostly plagioclase, with subordinate olivine).

Serpentinized rocks are classified on the basis of the original phase proportions present in the protolith, using the IUGS classification system (Streckeisen, 1973) for ultramafic rocks. For example, "serpentinized dunite" is a rock with 90% modal olivine originally present that has some specified proportion of serpentinization. Synoptic versions of the Leg 125 igneous/metamorphic VCD forms are published with this volume and are available on microfilm at all three ODP repositories.

Thin-Section Descriptions

Thin-section billets of igneous and metamorphic rocks are examined (1) to confirm the identity of petrographic groups in the cores, (2) to understand better the textures and interrelationships of the mineral phases, (3) to help define unit boundaries indicated by hand-specimen core descriptions, and (4) to define the secondary alteration mineralogy. Percentages of individual mineral phases are estimated and are reported on the detailed thin-section description sheets (Fig. 13). The terminology used for thin-section descriptions is used in the same manner as that for the macroscopic descriptions. In cases where discrepancies arose over the composition and abundance of mineral phases between hand-specimen and thin-section analyses, the thin-section descriptions are preferred.

X-Ray-Diffraction Analyses

A Philips ADP 3520 X-ray diffractometer is used for XRD analysis of mineral phases. Normal instrument conditions employ Cu Ka radiation with a nickel filter, 40 kV, 35 mA, a goniometer scan from 2° to 70° θ, a step size of 0.02°, and a count time of 1 s per step.

Normally, samples are ground using the Spex 8000 Mixer Mill or, when the sample is small, with an agate mortar and pestle. This material is then pressed into the sample holders or smeared on glass plates, which are placed in the sample holders for analysis.

Diffractograms are interpreted with the help of a computerized search and match routine using Joint Committee on Powder Diffraction Standards (JCPDS) powder files.

X-Ray-Fluorescence Analysis

Prior to analysis, samples are crushed in the Spex 8510 Shatterbox using a tungsten carbide barrel. This produces some Ta and massive W contamination of the sample. If post-cruise studies for these elements are envisaged using the shipboard XRF powders, and if time permits, samples are crushed using an agate-lined barrel.

A fully automated wavelength-dispersive ARL8420 XRF (3 kW) system equipped with an Rh target X-ray tube is used to determine the abundance of major oxides and trace elements in whole-rock samples. Analyses of the major oxides are performed using lithium borate glass disks doped with lanthanum as a "heavy absorber" (Norrish and Hutton, 1969). These disks are prepared from a mixture of 500 mg of rock powder, weighed after 2 hr of ignition at about 1030°C, and 6.000 g of dry flux, consisting of 80% lithium tetraborate and 20% La_2O_3. This mixture is then melted at 1150°C in a platinum-gold crucible for about 10 min and poured into a platinum-gold mold using a Claisse Fluxer. The 12:1 flux-to-sample ratio and the use of the lanthanum absorber make matrix effects insignificant over the normal range of igneous rock compositions. Hence, the following linear relationship between X-ray intensity and concentration is valid:

$$C_i = (I_i\, m_i)\, b_i ,$$

where C_i is the concentration of oxide i (wt%), I_i is the net peak X-ray intensity of oxide i, m_i is the slope of the

125-784A-37R-01 (6-9 cm) OBSERVER: SAB WHERE SAMPLED: Torishima Forearc Seamount, west flank

ROCK NAME: Serpentinized harzburgite

GRAIN SIZE: 0.05-5 mm

TEXTURE: Mesh and bastite

PRIMARY MINERALOGY	PERCENT PRESENT	PERCENT ORIGINAL	SIZE (mm)	COMPOSITION	MORPHOLOGY	COMMENTS
PHENOCRYSTS						
Olivine	2	80	0.1-0.5		Anhedral	Altered to serpentine mesh; wavy extinction.
Clinopyroxene	2	3	0.05-1		Anhedral	As exsolution lamellae (100) and as individual grains.
Spinel	1	2	0.05-1	Cr	Euhedral-anhedral	Red-brown; altering to magnetite.
Orthopyroxene	5	15	0.1-5		Subhedral-anhedral	Altered to serpentine bastite; kink-banded, wavy extinction, bent exsolution lamellae.
GROUNDMASS						
N/A	N/A	N/A	N/A		N/A	

SECONDARY MINERALOGY	PERCENT	REPLACING/ FILLING	COMMENTS
Clays	5	Serpentine	Dusty brown-black clay scattered throughout slide and intermixed with the serpentine.
Serpentine	69	Olivine, orthopyroxene	Mostly lizardite and/or chrysotile forming mesh and bastite textures.
Magnetite	15	Spinel, olivine, serpentine	Dusty 0.1-mm grains throughout slide and concentrated in veins (serpentine), mesh edges, and along cleavages.
Talc	1	Serpentine	Dusty, high birefringence; found associated with orthopyroxene and bastites in and along edges and cleavages.

VESICLES/ CAVITIES	PERCENT	LOCATION	SIZE (mm)	FILLING	SHAPE
Vesicles	0				

COMMENTS: Relatively pyroxene-rich harzburgite. Spinels are fractured with silicates forming between fractures. Some spinels form ragged elongate trains. Orthopyroxene are wavy and kink-banded; have inclusions of clinopyroxene and spinels(?). One orthopyroxene grain is split by 1 to 1.5-mm-wide serpentine veins. This slide has abundant magnetite mesh edges and in serpentine veins (which are almost all parallel throughout slide). This rock was further altered after serpentinization. No piece number given.

Figure 13. Thin-section description form used for metamorphic and igneous rock.

calibration curve for oxide i (wt%/cps), and b_i is the apparent background concentration for oxide i (wt%).

The slope m_i is calculated from a calibration curve derived from the measurement of well-analyzed reference rocks (BHVO-1, G-2, AGV-1, PCC-1, JGB-1, JP-1, BR, DR-N, UB-N). The background bi is determined either from blanks or is derived by regression analysis from the calibration curves.

Systematic errors resulting from short-term or long-term fluctuations in X-ray tube intensity are corrected by normalizing the measured intensities of the samples to those of a standard that is always run with a set of six samples. To reduce shipboard weighing errors, two glass disks are prepared for each sample. Accurate weighing is difficult on board the moving platform of the *Resolution*, and must be performed with particular care because weighing errors can be a major source of imprecision in the final analysis. Loss on ignition (LOI) values, if required, are determined by drying the sample at 110°C for 8 hr, and then by weighing before and after ignition at 1030°C.

Trace elements are determined by using pressed-powder pellets prepared by pressing (with 7 tons of pressure) a mixture of 5.0 g of dry rock powder (dried at 110°C for 2 hr) and 30 drops of polyvinyl alcohol binder into an aluminum cap. A modified Compton scattering technique, based on the intensity of the Rh Compton peak, is used for matrix absorption corrections (Reynolds, 1967).

An outline of the computation methods is as follows:

1. Input X-ray intensities. Dead-time corrected X-ray intensities are read into the program from an A.R.L. result file.

2. Correct drift. All peak and background intensities are corrected for machine drift by using a one-point correction of the form

$$D_i = S_i/M_i,$$

$$Id_i = I_iD_i,$$

where D_i is the drift factor for element i (generally 1.00 ± 0.01), S_i is the peak intensity for element i (measured on a synthetic standard, "POOP," at the time of calibration), M_i is the measured peak intensity for element i (measured on "POOP" at any time after the calibration), Id_i is the drift-corrected peak or background intensity for element i, and I_i is uncorrected peak or background intensity for element i.

3. Subtract backgrounds. Peak intensities are corrected for nonlinear backgrounds by measuring a peak-to-average background ratio for each element. This ratio is measured on synthetic and natural blank standards at the time of calibration using the following:

$$BF_i = PK_i/AVBg_i,$$

Table 2. X-ray-fluorescence analytical conditions, Leg 125.

Element	Line	Crystal	Detector[a]	Collimator	Peak (degrees)	Background offset (degrees)	Total count time (s) peak	Total count time (s) background
Major elements								
SiO_2	Kα	PET(002)	FPC	Coarse	109.25	0	40	0
TiO_2	Kα	LIF(200)	FPC	Fine	86.14	0	40	0
Al_2O_3	Kα	PET(002)	FPC	Coarse	145.27	0	100	0
[b]Fe_2O_3	Kα	LiF(200)	FPC	Fine	57.52	0	40	0
MnO	Kα	LiF(200)	KrSC	Fine	62.98	0	40	0
MgO	Kα	TLAP	FPC	Coarse	44.87	±0.80	200	200
CaO	Kα	LiF(200)	FPC	Coarse	113.16	0	40	0
Na_2O	Kα	TLAP	FPC	Coarse	54.71	−1.20	200	200
K_2O	Kα	LiF(200)	FPC	Fine	136.65	0	40	0
P_2O_5	Kα	Ge(111)	FPC	Coarse	140.94	0	100	0
Trace elements								
Rh	K-C	LiF(200)	Scint	Fine	18.59	0	100	0
Nb	Kα	LiF(200)	Scint	Fine	21.37	±0.35	200	200
Zr	Kα	LiF(200)	Scint	Fine	22.53	±0.35	100	100
Y	Kα	LiF(200)	Scint	Fine	23.78	±0.40	100	100
Sr	Kα	Lif(200)	Scint	Fine	25.13	±0.40	100	100
Rb	Kα	LiF(200)	Scint	Fine	26.60	±0.60	100	100
Zn	Kα	LiF(200)	Scint	Fine	41.79	±0.40	60	60
Cu	Kα	LiF(200)	Scint	Fine	45.02	±0.40	60	60
Ni	Kα	LiF(200)	Scint	Coarse	48.67	±0.60	60	60
Cr	Kα	LiF(200)	FPC	Fine	69.35	±0.50	60	60
Fe	Kα	LiF(220)	FPC	Fine	85.37	−0.40+0.70	40	40
V	Kα	LiF(220)	FPC	Fine	122.84	−0.50	60	60
TiO_2	Kα	LiF(200)	FPC	Fine	86.14	±0.50	40	40
[c]Ce	Lα	LiF(220)	FPC	Coarse	127.92	±1.50	100	100
[c]Ba	Lβ	LiF(220)	FPC	Coarse	128.53	±1.50	100	100

Note: All elements analyzed under vacuum on goniometer 1, at generator settings of 60 kV and 50 mA.
[a] FPC = flow proportional counter using P_{10} gas; KrSC = sealed krypton gas counter; Scint = NaI scintillation counter.
[b] Total iron as Fe_2O_3.
[c] Calibrated, but not analyzed for basalts.

where BF_i is the peak to average background ratio for element i, PK_i *is the peak intensity for element* i, and $AVBg_i$ is the average background intensity for element i.

Thus, when measuring unknowns, the true or modified background (MBg_i) is calculated by multiplying the average measured background for element i ($AVBg_i$) by the value of BF_i. This new modified background value is then subtracted from the peak intensity (PK_i) to arrive at the net peak intensity ($NETPK_i$) for element i:

$$MBg_i = AVBg_i\, BF_i,$$

$$NETPK_i = PK_i\, MBg_i.$$

4. Remove spectral interferences. During calibration, interferences are measured on synthetic pellets containing pure quartz and the interfering element. A ratio of the interference intensity to the net peak intensity of the interfering element is calculated and assumed constant with respect to concentration. When measuring an unknown sample, the net interference ($INTFER_{i,j}$) is calculated and removed by the following:

$$INTFER_{i,j} = NETPK_i\, IR_{i,j},$$

$$CNETPK_j = NETPK_j\, INTFER_{i,j},$$

where $INTFER_{i,j}$ is the net interference intensity of element i on element j, and $CNETPK_j$ is the net intensity of element j with the interference element i removed. In the case of mutually interfering elements, an iterative approach to this same calculation is used until all the involved elements converge on their respective corrected values. 5. Measure mass absorption coefficients. To correct for matrix differences between samples, three separate mass absorption coefficients are determined following a modification of the Compton scattering technique of Reynolds (1967). Measured intensities from the Rh K-series Compton, Fe Ka, and Ti Ka lines are compared to the calculated absorption coefficients of rubidium (ARb), chromium (ACr), and vanadium (AV), respectively. From this comparison, three equations can be written to describe the relationship between each coefficient and its respective line. The three equations derived from the Leg 111 calibration are as follows:

$$A_{Rb} = 104/([Rhcps\ 0.0698] + 57.79),$$

$$A_{Cr} = A_{Rb}/([Fecps\ 1.044 \times 10^{-6}] + 0.081),$$

$$A_V = A_{Cr}/([Ticps 6.140 \times 10^{-6}] + 0.778)$$

where *Rhcps*, *Fecps*, *Ticps* are the intensities in counts per second of the Rh Compton, Fe Ka, and Ti Ka lines, respectively. Using this method, unknowns can be measured and corrected for matrix differences without calculating the absorption coefficients for each sample.

6. Calculate concentrations. Once all spectral and matrix corrections are calculated, the equation for calculating elemental concentrations is reduced to

$$C_i = (CNETPK_i A_i)/K_i,$$

where C_i is the concentration of element i in parts per million, $CNETPK_i$ is the corrected net peak intensity for element i, A_i is the mass absorption coefficient for element i, and K_i is the calibration factor (ppm/cps) for element i. K_i is analogous to the calibration curve slope (mi) for major elements and is determined in the same manner for natural rock (AGV-1, UB-N, G-2, BHVO-1, RGM-1, DRN) and synthetic (com-

pressed, spiked quartz powders) standards. Details of the analytical conditions for each element determined are given in Table 2.

PHYSICAL PROPERTIES

The shipboard physical-properties program provides measurements of the different physical or geotechnical properties of sampled materials. The physical properties routinely measured on board *Resolution* are bulk density, grain density, water content, porosity, compressional-wave velocity, magnetic susceptibility, thermal conductivity, and undrained shear strength. Physical properties assist in the characterization of different lithologic units, allow for verification of downhole geophysical logging results, and can provide constraints on the interpretation of seismic-reflection and other geophysical data. Furthermore, these data may be used to estimate the permeability and degree of consolidation, to correct sedimentation rates, and to aid in heatflow calculations. Depth profiles of geotechnical properties may be used to distinguish lithologic boundaries at drill sites as well as to correlate and establish facies changes between sites.

A discussion of physical-property determination with respect to equipment, methods, errors, correction factors, and problems related to coring disturbance was presented by Boyce (1976), who showed that physical properties are influenced by drilling and sampling disturbance, as well as by the testing procedures used in the laboratory. For example, the water content of a particular sample may be increased by the drilling fluid (seawater) that typically surrounds a disturbed core for many hours prior to removal of the sample from the core for testing.

Samples used for determining physical properties were selected from areas having the least sample disturbance, and sufficient samples were tested to permit us to characterize the major lithologic units. Typically, one sample was taken per section of core for evaluating index properties; compressional-wave velocity was measured on the same sample or on one from the immediate vicinity. Samples were chosen to be as representative as possible of the section as a whole; however, a few samples were taken from thinner units having markedly different lithologies. Sample selection and relative frequency depended on the thickness and homogeneity of a particular sequence.

The testing methods employed during Leg 125 are discussed in the following text in the order in which they were performed on each core. GRAPE, compressional-wave (*P*-wave) velocity logging, magnetic susceptibility, and the determination of thermal conductivity of soft sediments were performed on whole-round core samples. Other measurements were conducted on discrete samples of split cores.

Gamma-Ray Attenuation Porosity Evaluator

The GRAPE technique was described by Boyce (1976). The GRAPE makes a continuous measurement of wet-bulk density on whole APC and XCB sections. Generally, piston cores and only the first few XCB cores were tested because GRAPE data are valid only from complete cores. An aluminum standard was used to calibrate the apparatus and was analyzed frequently. The section to be measured was mounted horizontally on the MST, while the core moved through the sensors on a conveyor belt. The attenuation of gamma rays passing through the liner and core was measured every 1.5 to 2.0 cm, and the bulk density was calculated from the attenuation values. GRAPE data were filtered to remove data that result from gas or gaps and end-cap effects before the data were averaged over 0.2- or 0.5-m intervals. All bulk-density data are reported in units of g/cm^3.

P-Wave Logger

The *P*-wave logger (PWL) operates on the MST along with the GRAPE and magnetic susceptibility meter. A transducer produced a short 500-kHz compressional-wave pulse at a repetition rate of 1 kHz. A receiving transducer was positioned so that the two transducers were aligned perpendicular to the core axis. A pair of displacement transducers monitored the separation between the compressional-wave transducers. This compensated for variations in the outside liner diameter without degrading the accuracy of the velocities measured. Measurements were performed at 1.5- to 2.0-cm intervals.

Water was applied to the core liner to improve acoustic contact between the transducers and the liner. As with the GRAPE, only APC and the first few XCB cores were measured because high-quality data can only be obtained from cores that completely fill the liner. The deeper XCB cores and all RCB cores from Leg 125 contained annular voids between the core and the inside of the liner that prevented transmission of the compressional waves between the transducers. Filtering the PWL data removed data resulting from gas, gaps, and end-cap effects. Weak returns with signal strengths below a threshold value of 200 m/s were not recorded. The data were averaged over 0.2- or 0.5-m intervals.

Magnetic Susceptibility

Magnetic susceptibility was measured on the MST. Poor data were recorded for Sites 778 and 779 because of sensor malfunction and improper zeroing of the instrument. Prior to Site 780, the sensor was replaced and functioned well. Like GRAPE and PWL data, magnetic susceptibility data are only valid from full core liners. Erratic values have been observed when liners are only partially filled or contain broken pieces of hard rock. Magnetic susceptibility is dimensionless in the SI system.

Thermal Conductivity

Following MST measurements and prior to measuring thermal conductivity, the whole-round cores were equilibrated to room temperature for 2 to 4 hr. The thermal-conductivity techniques used here have been described by Von Herzen and Maxwell (1959) and Vacquier (1985). All thermal-conductivity data are reported in units of W/mK.

Soft-Sediment Thermal Conductivity

Needle probes connected to a Thermcon-85 unit were inserted into the sediment through holes drilled into the core liner, and the thermal drift was monitored. Probe behavior was monitored by inserting an additional probe into a reference material. Once the temperature became stable, the probes were heated, and the coefficient of thermal conductivity was calculated as a function of the change in resistance in the probe. When the sediment became too stiff to allow for easy insertion of the probe, holes were drilled into the core material. We attempted to insert the probes at locations along each core section that appeared to be the least disturbed. However, an annulus of disturbed sediment and drill fluid that was commonly present along the inside of the liner prevented some visual identification of the more intact segments of the core.

Hard-Rock Thermal Conductivity

Thermal conductivity measurements on well-lithified sediments and rocks were performed on split cores using a needle probe that was partially embedded in a slab of insulating material. The split-core sample was not polished. The flat surface of a selected sample of split core was placed on top of

the slab. Dow Corning 3 silicone was used to improve the thermal contact between the slab and the sample. The sample and slab were immersed in a salt-water bath and allowed to equilibrate thermally. The probe was heated, and measurements of changes of resistance in the probe were performed every 9 s for a 9-min interval. Thermal conductivity was determined from the most linear portion of a temperature vs. log-time plot.

Undrained Shear Strength

Undrained shear strength of the sediment (Boyce, 1977; Lee, 1984) was determined using a Wykeham-Farrance motorized vane apparatus. This four-bladed vane has a diameter of 1.28 cm and is 1.28 cm long. It was inserted into the split section perpendicular to the core axis until the top of the blade was covered by about 4 to 6 mm of sediment. The vane was then rotated at a rate of about 90°/min until the sediment failed. The undrained shear strength was calculated from the peak torque obtained at failure. Vane rotation continued for a minimum of 120° to permit determination of remolded shear strength. The peak and remolded "torques" were measured from calibrated plots of torque vs. rotation generated on a Hewlett-Packard 7015B X-Y Recorder. Vane testing ceased when radial cracking or other noncylindrical failure surfaces developed around the vane. During Leg 125, noncylindrical failures were observed in the stiffer sediments that had undrained shear strengths exceeding approximately 50 kPa. All shear strengths are reported in units of kPa.

Compressional-Wave Velocity

Compressional-wave velocities, in addition to those previously described, were measured on samples that were sufficiently stiff to allow for sampling and to provide adequate signal strength. Velocities were calculated from the determination of the traveltime of a 500-kHz compressional wave through a measured thickness of sample, using a Hamilton Frame Velocimeter and Tektronix DC 5010 counter/timer system. Travel distance was measured with an attached variable resistor (LVT) connected to a Tektronix DM 5010 digital multimeter. Parallel-sided samples were cut either with a knife in the softer sediments or with a double-bladed diamond saw in the more brittle or lithified sediments. Samples of igneous and metamorphic rocks were cut with a double-bladed diamond saw or a 2.5-cm rock corer.

The Hamilton Frame velocity transducers were calibrated with lucite and aluminum standards. The variable resistor was calibrated with standard lengths of aluminum cylinders. Zero traveltimes were measured with the two transducers in contact with the signal amplitude adjusted to 2 V on the oscilloscope. Zero times were determined once per core tested. Seawater was used to improve the acoustic contact between the sample and the transducers. Readings of traveltime through samples were taken after the signal amplitude on the oscilloscope had been adjusted to 2 V. When signal strength was insufficient, velocities from the sample were not recorded.

Index Properties

The index properties of wet-bulk density, grain density, porosity, water content, and void ratio were determined on selected samples of sediment and rock. Measuring index properties and compressional-wave velocities from the same samples allowed us to correlate directly among those values that may indicate trends as well as to provide a check for data consistency. Samples were weighed wet using two calibrated Scientech 202 electronic balances interfaced with a PRO350 computer, which compensates for the motion of the ship by taking the average of 200 sample weighings. Dry-sample weight was determined using the same procedure after freeze-drying the sample for at least 12 hr. Dry volumes were measured using a Quantochrome Helium Penta-Pycnometer. The pycnometer was not accurate for wet volumes because of helium absorption by water. Therefore, wet volumes were calculated based on the assumed volume of water extracted from the sample using the following expression:

(wet weight dry weight/density of seawater) + dry volume,

using a value of 1.03 g/cm^3 as the density of seawater.

The following definitions and units were used for the index properties:

1. Porosity (%) = 100 × volume of water/volume of wet sediment.
2. Bulk density (g/cm^3) = weight of wet sediment/volume of wet sediment.
3. Grain density (g/cm^3) = weight of dry sediment/volume of dry sediment.
4. Water content (%) = 100 × weight of water/dry weight of sediment.
5. Void ratio (dimensionless) = volume of water/volume of dry sediment.

Dry-sediment weights and volumes used in the preceding calculations were corrected for salt content (assuming seawater salinity of 35‰) by subtracting the estimated weight and volume of residual salt.

Data Presentation

The physical properties measured for samples during Leg 125 are presented in tables and figures in each site chapter. All index properties and thermal-conductivity data are presented in both the tables and the figures. (Tables of GRAPE and PWL data would be excessively long, however, and thus are not presented.) The GRAPE, PWL, and magnetic susceptibility data were filtered to remove spurious data and to reduce the number of data points. Porosity (j), bulk density (r),and compressional-wave velocity (V*p*) values are given in the "Physical Properties" column on the barrel sheets for the cores of each site.

DOWNHOLE MEASUREMENTS

Tool Strings

Downhole logging directly determines the physical and chemical properties of formations adjacent to the borehole. Interpretation of these continuous, *in-situ* measurements can provide a stratigraphic, lithologic, geophysical, and mineralogic characterization of the site. After coring is completed at a hole, a tool string is lowered downhole on a seven-conductor cable, and each of several tools in the tool string continuously monitors some property of the adjacent borehole. Of the dozens of different tool strings commonly used in the petroleum industry, two Schlumberger tool strings were used during Leg 125: the seismic stratigraphic and lithoporosity (physical properties) string and the geochemical string. The Lamont-Doherty Geological Observatory (LDGO) borehole televiewer (BHTV) and magnetometer also were run during Leg 125.

The seismic-lithoporosity (physical properties) combination used during Leg 125 is a digital string, normally consisting of the LDGO temperature tool (TLT), the dual induction tool (DIT), the digital sonic tool (SDT), the mechanical caliper device (MCD), and the lithodensity tool (LDT). This tool

combination measures compressional-wave velocity and can provide indicators of the two variables that most often control velocity: porosity, as indicated by resistivity, and clay content. This combination can also provide measurements of formation porosity and density and can determine the spectral content of naturally occurring radiation.

The geochemical combination normally consists of the LDGO temperature tool, the compensated neutron tool (CNT), the induced gamma-ray spectrometry tool (GST), the aluminum clay tool (ACT), the natural gamma-ray spectrometry tool (NGT), and the general purpose inclination tool (GPIT). This tool combination can measure the relative concentrations of 11 elements: silicon, calcium, aluminum, iron, sulfur, manganese, hydrogen, chlorine, potassium, thorium, and uranium.

Logs

A brief description of the logging tools run during Leg 125 is provided. The principles and applications of logging tools have been described in detail in Schlumberger (1972), Serra (1984), and Timur and Toksöz (1985).

Temperature Tool

The LDGO temperature tool (TLT) is a self-contained tool that can be attached to any Schlumberger tool string or to the televiewer. Data from two thermistors and a pressure transducer were collected every 0.5 to 5.0 s and stored in a Tattletale computer within the tool. Following the logging run, data are dumped from the Tattletale to the Masscomp computer for analysis. A fast-response thermistor, although not too accurate, is able to detect sudden very small temperature excursions caused by fluid flow from the formation. A slow-response thermistor is very accurate and can be used to estimate heat flow. Data are recorded as a function of time; conversion to depth can be based on the pressure transducer or, preferably, on simultaneous recording by Schlumberger of both depth and time.

Electrical Resistivity

The dual induction tool (DIT) provides three different measurements of electrical resistivity, each with a different depth of investigation. Two induction devices (deep and medium resistivity) send high-frequency alternating currents through transmitter coils, creating magnetic fields that induce secondary (Foucault) currents in the formation. These ground-loop currents produce new inductive signals, proportional to the conductivity of the formation, which are recorded by the receiving coils. Measured conductivities then can be converted to resistivity. A third device (spherically focused resistivity) can measure the current necessary to maintain a constant voltage decrease across a fixed interval. Vertical resolution is approximately 2 m for the medium- and deep- resistivity devices and 1 m for the focused-resistivity device.

Water content and salinity are by far the most important factors controlling the electrical resistivity of rocks. To the first order, resistivity responds to the inverse square root of porosity (Archie, 1942). Other factors influencing resistivity include the concentration of hydrous and metallic minerals, vesicularity, and geometry of interconnected pore space.

Sonic Velocity

The digital sonic (SDT) tool uses two acoustic transmitters and two receivers to measure the time required for sound waves to travel over source-receiver distances of 2.4, 3.0, and 3.6 m. The raw data are expressed as time required for a sound wave to travel through 0.30 m of formation; these traveltimes are then converted to sonic velocities. First arrivals for the individual source-receiver paths can be used to calculate the velocities of the different waves traveling in the formation (compressional, shear, etc.). Only compressional-wave velocity is determined during data acquisition, but waveforms are recorded for post-cruise determination of shear-wave velocities and possibly to improve compressional-wave velocities. The vertical resolution of the tool is 0.30 m. Compressional-wave velocity is dominantly controlled by porosity and lithification; decreases in porosity and increases in lithification cause the velocity to increase.

Mechanical Caliper Device The mechanical caliper device (MCD) can provide a basic two-dimensional caliper log of the borehole by means of a bowspring-mounted measurement system. The hole diameter (HD) log is used to detect washouts or constrictions. Borehole diameter significantly affects many of the other logging measurements, and thus is an important factor in log correction routines.

Lithodensity Tool

The lithodensity tool (LDT) uses a ^{137}Ce gamma-ray source to measure the resulting flux at fixed distances from the source. Under normal operating conditions, attenuation of gamma rays is chiefly caused by Compton scattering (Dewan, 1983). Formation density is extrapolated from this energy flux by assuming that the atomic weight of most rock-forming elements is approximately twice the atomic number. An index of photoelectric effect is also provided. Photoelectric absorption occurs in the energy window below 150 keV and depends on the energy of the incident gamma ray, the atomic cross section, and the nature of the atom. This measurement is almost independent of porosity, thus can be used directly as a matrix lithology indicator. The radioactive source and detector array were placed in a tool that was pressed against the borehole wall by a strong spring. Excessive roughness of the hole may cause some drilling fluid to infiltrate between the skid and the formation. As a consequence, density readings can be artificially low. Approximate corrections can be applied by using caliper data. The vertical resolution is about 0.30 m.

Compensated Neutron Porosity

A radioactive source mounted on the compensated neutron porosity tool (CNT) sonde emits fast neutrons (4 MeV) into the formation, where they are scattered and slowed by collisions with other nuclei. When the neutrons reach a low energy level (0.025 MeV), they are captured and absorbed by atomic nuclei, such as hydrogen, chlorine, silicon, and boron. The scattering cross section is the quantity that describes the rate at which neutrons were slowed. The scattering cross section for hydrogen is about 100 times larger than for any other common element in the crust, so most energy dissipation is caused by collisions with water molecules. Therefore, a change in the number of neutrons detected at a receiver can be related to porosity. In practice, an array of detectors is used to minimize borehole or drilling fluid effects. Because water is present both in pores and as bound water (e.g., clay minerals), porosity measurements made in the presence of hydrous minerals overestimate the true porosity. The vertical resolution of the tool theoretically is about 0.25 m, but low signal-to-noise ratio degrades the potential resolution.

Gamma-Ray Spectrometry Tool

The induced gamma-ray spectrometry tool (GST) consists of a pulsed source of 14-MeV neutrons and a gamma-ray scintillation detector. A surface computer performs spectral

analysis of gamma rays resulting from the interactions of neutrons emitted by the source with atomic nuclei in the formation. Characteristic sets of gamma rays from six elements dominate the spectrum: calcium, silicon, iron, chlorine, hydrogen, and sulfur. Processing normalizes the sum of these data, so they do not reflect the actual elemental composition. Therefore, ratios of these elements commonly are used for interpreting the lithology, porosity, and salinity of formation fluid.

Aluminum Clay Tool

Aluminum abundance, as measured by the aluminum clay tool (ACT), is determined by neutron-induced (Californium chemical source) late gamma-ray spectrometry. By placing NaI detectors both above and below the neutron source, contributions from natural gamma-ray activity can be removed. Calibration to elemental weight percent is performed by taking irradiated core samples of known volume and density and measuring their gamma-ray output while placed in a jig attached to the logging tool (typically after logging).

Natural Gamma Ray Tool

The natural gamma-ray tool (NGT) measures the natural radioactivity of the formation. Most gamma rays are emitted by the radioactive isotope ^{40}K and by the radioactive elements of the uranium and thorium series. The gamma-ray radiation originating in the formation near the borehole wall is measured by a scintillation detector mounted inside the sonde. Analysis is achieved by subdividing the entire incident gamma-ray spectrum into five discrete energy windows. The total counts recorded in each window, for a specified depth in the well, are processed at the surface to give the elemental abundances of potassium, uranium, and thorium. Because radioactive elements tend to be most abundant in clay minerals, the gamma-ray curve is commonly used to estimate the clay or shale content. There are rock matrices, however, for which the radioactivity ranges from moderate to extremely high values, as a result of the presence of volcanic ash, potassic feldspar, or other radioactive minerals.

General Purpose Inclination Tool

The general purpose inclination tool (GPIT) contains three accelerometers at right angles to each other and three magnetometers, also at right angles to each other. The device measures the orientation of the tool string within the hole and the orientation (or deviation) of the borehole itself. Several other engineering measurements are also performed.

Borehole Televiewer

The borehole televiewer (BHTV) is an ultrasonic, high-resolution logging tool designed to measure the geometry of the borehole wall, fractures, and lithostratigraphic features. The televiewer contains a rotating acoustic transducer that emits a focused 3° beam pulse at a rate of 1800 times/s. Two transducers allow the BHTV to operate in either low-frequency (400 kHz) or high-frequency (1.4 MHz) mode. The high-frequency transducer is designed to resolve such detailed features as fracture density and fracture aperture. The low-frequency transducer emits a more powerful signal and thus is usually more useful in the large-diameter ODP holes. The orientations of all features are determined by a fluxgate magnetometer that triggers the signal at each crossing of magnetic north, while the tool is pulled uphole at a rate of 2.5 cm/s. A reflectance image of the borehole wall is obtained in real time by windowing the acoustic reflection off the borehole wall and recording this on Polaroid film. The raw output consists of full waveform acoustic seismograms that also are recorded on videotape for later reprocessing. The traveltimes and the degree of acoustic reflectance from these data can then be used to determine a more accurate three-dimensional image of the borehole geometry, as well as to delineate the textural characteristics of the borehole wall.

Quality of Log Data

The quality of log data may be seriously degraded in excessively large sections of the borehole or by rapid changes in the hole diameter. Resistivity and velocity measurements are least sensitive to borehole effects. The nuclear measurements (i.e., density, neutron porosity, and both natural and induced spectral gamma rays) are most seriously impaired because of the large attenuation by the borehole fluid. Corrections can be applied to the original data to reduce the effects of these conditions and, generally, to reduce any departure from the conditions under which the tool was calibrated.

There may be small deviations in depth between different logs. These deviations are caused by either stretching of the cable or heave of the ship during recording. Small errors in correlation can impair the interpretations in zones of frequent changes of lithology. To minimize such errors, a hydraulic heave compensator adjusts for rig motion in real time. Precise correlation between logging depths and depth of features within the cores is not possible in zones where core recovery is low because of the inherent ambiguity of placing the recovered section within the interval cored.

Log Analysis

During logging, incoming data are observed in real time on a monitor oscilloscope and recorded simultaneously on digital tape in either the Schlumberger logging unit or the downhole measurements laboratory. After logging, the Schlumberger tape is read by the Masscomp computer system in the laboratory and reformatted to a file format compatible with the Terralog log-interpretation software package. Rather than being a "black box," Terralog is an interactive system that consists of many log manipulation and plotting options. Thus, log analysis and interpretation vary in duration and procedure for each site. Most log interpretation was conducted aboard ship; logs will be analyzed and interpreted further after the cruise, using a companion system in the Borehole Research Laboratory of Lamont-Doherty Geological Observatory.

Reprocessing of Logs

Raw count rates for six elements (calcium, silicon, iron, sulfur, chlorine, and hydrogen) are obtained in real time by the Schlumberger data acquisition software. These count rates commonly exhibit some inversion interference of chlorine with other elemental count rates, which is manifest as a strong, but spurious, correlation between chlorine and calcium, and weaker correlations with other elements measured by the tool. This interference, which has been attributed to the dominance of the induced gamma-ray spectrum by chlorine, is unavoidable in ODP holes because the minimum pipe diameter is too small to allow for use of a boron sleeve to suppress chlorine counts. Most of the effects of this interference are removed aboard ship by adding to each count-rate log the product of chlorine counts and the slope of a first-degree regression with chlorine.

The shipboard correction is obviated by post-cruise reprocessing, using a Schlumberger Elite 1000 work station and proprietary Schlumberger software. With a revised algorithm, the gamma-ray spectrum at each depth is inverted for titanium, gadolinium, and potassium in addition to the six ele-

ments previously listed. Though gadolinium is present in concentrations of only a few parts per million, its neutron-capture cross section is so large that gadolinium can account for 10% to 30% of the total gamma-ray spectrum. Inclusion of these additional elements improves the quality of the overall inversion, particularly by improving the accuracy of calculated abundance of calcium, by converting sources of unaccounted variance to signals. However, the determined potassium concentrations are less accurate than those from the NGT, and the hydrogen concentrations are less accurate than those from the neutron tool.

Aluminum concentrations from the ACT require only one correction, an adjustment for variations in cable speed. Changes in logging speed affect the time lag between neutron irradiation of the formation and recording of the induced gamma-ray spectrum because the number of induced gamma rays decreases rapidly with time. Post-cruise correction will be made on the basis of the cable speed recorded during logging. However, the small amount of ship heave during logging may make this correction less reliable in ODP holes than in land wells.

When both Schlumberger tool strings are run, further reprocessing of geochemical logs is possible. The relative abundances of calcium, silicon, iron, titanium, aluminum, sulfur, potassium, thorium, uranium, and gadolinium are used to calculate a log of predicted photoelectric effect. The difference between this log and the actual log of photoelectric effect can be attributed to the only two major elements not measured directly, magnesium and sodium. Major elements are converted from volume percent to weight percent using logs of total porosity (bound water plus pore water) and density. Major elements are expressed in terms of oxide dry weight percent, based on the assumption that oxygen is 50% of the total dry weight.

If GST data are available, but not enough log types are run to permit complete solution for oxide weight percentage, one further processing step is made. Omitting chlorine and hydrogen, the yields of the other GST elements (calcium, silicon, iron, titanium, sulfur, potassium, and gadolinium) are summed, and each is expressed as a fraction of this total yield. This procedure corrects for variation porosity and count rate. Although the absolute abundance of each element is not determined, downhole variations in relative abundance are indicated.

Sonic logs obtained in real time are not based on full-waveform analysis, but on a threshold-measuring technique that attempts to detect the compressional-wave arrival by a first-break criterion. Sometimes this technique fails and either the threshold is exceeded by noise or the first compressional arrival is below the threshold. This phenomenon, called cycle skipping, creates spurious spikes on the sonic log. During Leg 125, raw traveltimes were reprocessed with an algorithm designed to reject cycle skips (Srivastava, Arthur, et al., 1987). This algorithm was expanded to include calculation of a caliper log, based on Snell's law and the fact that the observed total source-receiver traveltime is a sum of the known refracted-wave traveltime through the formation and unknown traveltime in the borehole. Though the resulting caliper log is sensitive to assumed fluid velocity, it is probably superior to the hole diameter measured by the caliper tool. The caliper tool used at ODP is subject to sticking when formation mud gets into its mechanical parts, resulting in bimodal (fully open or nearly fully closed) readings.

Synthetic Seismograms

Synthetic seismograms are generated from logging data obtained with the long-spaced sonic (LSS) tool. The bulk-density log from the lithodensity tool or a pseudodensity log created from other logs is required in addition to the slowness log. In many cases, a simple constant density log can be used. Experience shows that this often gives surprisingly good results because both velocity and density are usually controlled by the same parameter: porosity. When velocity and density are highly correlated, synthetic seismograms using a constant density log or an actual density log are virtually identical.

The slowness and density logs are used in the program to generate an impedance log (velocity × density), which is convolved with a zero-phase Ricker wavelet. The frequency of this wavelet can be varied, depending on the source generating the original seismic profile. A 30-Hz wavelet is capable of a vertical resolution on the order of 30 m, so reflectors cannot generally be attributed to any small-scale lithologic horizons. The synthetic seismogram is plotted with two-way traveltime on the left scale and depth below seafloor on the right. The plot is scaled to uniform time spacing, not uniform depth spacing.

In-Situ Stress Measurements

The BHTV is used to detect stress directions from borehole breakouts. Stress-induced wellbore breakouts are elongated zones of spalling along cylindrical holes in rocks. They commonly span a few tens of degrees of circumference. In an isotropic, linearly elastic rock subject to differential stresses, breakouts form along the borehole wall as a result of compressive stress concentrations exceeding the strength of the rock. Under these conditions, the breakout orientation will develop in the direction of the least dominant horizontal stress. Research has demonstrated in different areas that stress orientations deduced from breakouts are consistent with other independent indicators (Bell and Gough, 1979; Zoback and Zoback, 1980, in press; Zoback et al., 1988). Differential horizontal stresses that do not cause failure of the borehole wall may cause borehole ellipticity. Ellipticity also can be detected with the BHTV.

REFERENCES

Archie, G. E., 1942. The electrical resistivity log as an aid in determining some reservoir characteristics. *J. Pet. Technol.*, 5:1–8.

Backman, J., Duncan, R. A., et al., 1988. *Proc. ODP, Init. Repts.*, 115: College Station, TX (Ocean Drilling Program).

Barnes, R. O., 1988. ODP *in-situ* fluid sampling and measurement: a new wireline tool. *In* Mascle, A., Moore, J. C., et al., *Proc. ODP, Init. Repts.*, 110: College Station, TX (Ocean Drilling Program), 55–63.

Barron, J. A, 1983. Latest Oligocene through early middle Miocene diatom biostratigraphy of the eastern tropical Pacific. *Mar. Micropaleontol.*, 7:487–515.

_____, 1985a. Late Eocene to Holocene diatom biostratigraphy of the equatorial Pacific Ocean, Deep Sea Drilling Project Leg 85. *In* Mayer, L., Theyer, F., et al., *Init. Repts. DSDP*, 85: Washington (U.S. Govt. Printing Office), 413–456.

_____, 1985b. Miocene to Holocene planktic diatoms. *In* Bolli, H. M., Saunders, J. B., and Perch-Nielsen, K. (Eds.), *Plankton Stratigraphy*: Cambridge (Cambridge Univ. Press), 763–810.

Bell, J. S., and Gough, D. I., 1979. Northeast-southwest compressive stress in Alberta: evidence from oil wells. *Earth Planet. Sci. Lett.*, 45:475–482.

Berggren, W. A., 1977. Atlas of Paleogene planktonic foraminifera. *In* Ramsey, A.T.S. (Ed.), *Oceanic Micropaleontology* (vol. 1): London (Academic Press), 205–300.

Berggren, W. A., Kent, D. V., Flynn, J. J., and Van Couvering, J. A., 1985. Cenozoic geochronology. *Geol. Soc. Am. Bull.*, 96:1407–1418.

Blow, W. H., 1969. Late Middle Eocene to Recent planktonic foraminiferal biostratigraphy. *In* Renz, H. H., and Br×nnimann,

P. (Eds.), *Proc. Int. Conf. Planktonic Microfossils*, Geneva, 1967, 1:199–422.

_____, 1979. *The Cainozoic Foraminiferida*: Leiden (E. J. Brill).

Boyce, R. E., 1976. Definitions and laboratory techniques of compressional sound velocity parameters and wet-water content; wet bulk density and porosity parameters by gravimetric and gamma ray attenuation techniques. *In* Schlager, S. O., Jackson, E. D., et al., *Init. Repts. DSDP*, 33: Washington (U.S. Govt. Printing Office), 931–958.

_____, 1977. Deep-sea drilling procedures for shear strength measurements of clayey sediment using modified Wykeham Farrance Laboratory Vane Apparatus. *In* Barker, P., Dalziel, I.W.D., et al., *Init. Repts. DSDP*, 36: Washington (U.S. Govt. Printing Office), 1059–1068.

Bramlette, M. N., and Bradley, W. H., 1942. Geology and biology of North Atlantic deep-sea cores between Newfoundland and Ireland. Pt. 1, lithology and geologic interpretations. *U.S. Geol. Surv. Prof. Pap.*, 196(A):1–55.

Bukry, D., 1973. Low-latitude coccolith biostratigraphic zonation: DSDP Leg 15. *In* Edgar, N. T., Saunders, J. B., et al., *Init. Repts. DSDP*, 15: Washington (U.S. Govt. Printing Office), 685–703.

Burckle, L. H., 1972. Late Cenozoic diatom zones from the eastern equatorial Pacific. *Nova Hedwigia*, 39:217–246.

_____, 1977. Pliocene and Pleistocene diatom datum levels for the equatorial Pacific. *Quat. Res.*, 7:330–340.

_____, 1978. Early Miocene to Pliocene diatom datum levels for the equatorial Pacific. *Proc. 2nd Working Group Mtg., Biostratigraphic Datum-Planes of the Pacific Neogene, IGCP Project 114*, 1:25–44.

Burckle, L. H., and Trainer, J., 1979. Middle and late Pliocene diatom datum levels from the central Pacific. *Micropaleontology*, 25(3):281–293.

Cowan, D. S., and Mansfield, C. F., 1970. Serpentinite flows on Joaquin Ridge, Southern Coast Ranges, California. *Geol. Soc. Am. Bull.*, 81:2615–2628.

Dewan, J. T., 1983. *Essentials of Modern Open-Hole Log Interpretation*: Tulsa (Pennwell Books).

Fisher, R. V., and Schmincke, H.-U., 1984. *Pyroclastic Rocks*: New York (Springer-Verlag).

Gealy, E. L., Winterer, E. L., and Moberly, R. M., Jr., 1971. Methods, conventions, and general observations. *In* Winterer, E. L., Riedel, W. R., et al., *Init. Repts. DSDP*, 7, Pt. 1: Washington (U.S. Govt. Printing Office), 9–26.

Gieskes, J. M., and Peretsman, G., 1986. *Water Chemistry Procedures Aboard JOIDES Resolution - Some Comments*. Ocean Drilling Program, Tech. Note 5.

Kennett, J. P., and Srinivasan, M. S., 1983. *Neogene Planktonic Foraminifera: A Phylogenetic Atlas:* Stroudsburg, PA (Hutchinson Ross).

Koizumi, I., 1986. Pliocene and Pleistocene diatom datum levels related with paleoceanography in the northwest Pacific. *Mar. Micropaleontol.*, 10:309–325.

Lee, H. J., 1984. State of the art: laboratory determination of strength of marine soils. *In* Chaney, R. C., and Demars, K. R. (Eds.), *Strength Testing of Marine Sediments: Laboratory and In-Situ Measurements*. ASTM Spec. Tech. Publ., 883:181–250.

Manheim, F. T., and Sayles, F. L., 1974. Composition and origin of interstitial waters of marine sediments based on deep sea drill cores. *In* Goldberg, E. D. (Ed.), *The Sea* (vol. 5): New York (Wiley), 527–568.

Martini, E., 1971. Standard Tertiary and Quaternary calcareous nannoplankton zonation. *In* Farinacci, A. (Ed.), *Proc. 2nd Plankton. Conf., Roma 1970*, 2:739–785.

Moberly, R., and Klein, G. de V., 1976. Ephemeral color in deep-sea cores. *J. Sediment. Petrol.*, 46:216–225.

Munsell Soil Color Charts, 1975. Baltimore (Munsell Color).

Norrish, K., and Hutton, J. T., 1969. An accurate X-ray spectrographic method for the analysis of a wide range of geological samples. *Geochim. Cosmochim. Acta*, 33:431–453.

Okada, H., and Bukry, D., 1980. Supplementary modification and introduction of code numbers to the low-latitude coccolith biostratigraphic zonation. *Mar. Micropaleontol.*, 5(3):321–325.

Reynolds, R. C., 1967. Estimations of mass absorption coefficients by Compton scattering: improvements and extensions of the method. *Am. Mineral.*, 48:1133–1143.

Schmid, R., 1981. Descriptive nomenclature and classification of pyroclastic deposits and fragments: recommendations of the IUGS Subcommission on the Systematics of Igneous Rocks. *Geology*, 9:41–43.

Schlumberger Ltd., 1972. *Log Interpretation* (vol. 1): Houston.

Serra, O., 1984. *Fundamentals of Well Log Interpretation*: Amsterdam (Elsevier).

Shepard, F. P., 1954. Nomenclature based on sand-silt-clay ratios. *J. Sediment. Petrol.*, 24:151–158.

Shipboard Scientific Party, 1988. Explanatory Notes: Leg 112. *In* Suess, E., von Huene, R., et al., *Proc. ODP, Init. Repts.*, 112: College Station, TX (Ocean Drilling Program), 25–44.

Srivastava, S., Arthur, M. A., et al., 1987. Site 645. *In* Srivastava, S., Arthur, M. A., et al., *Proc. ODP, Init. Repts.*, 105: College Station, TX (Ocean Drilling Program), 61–418.

Streckeisen, A. L., 1973. Plutonic rocks: classification and nomenclature recommended by the IUGS Subcommission on the Systematics of Igneous Rocks. *Geotimes*, 18–10:26–30.

Timur, A., and Toksöz, M. N., 1985, Downhole geophysical logging. *Annu. Rev. Earth Planet. Sci.*, 14:315–344.

Vacquier, V., 1985. The measurement of thermal conductivity of solids with a transient linear heat source on the plane surface of a poorly conducting body. *Earth Planet. Sci. Lett.*, 74:275–279.

Von Herzen, R. P., and Maxwell, A. E., 1959. The measurement of thermal conductivity of deep-sea sediments by a needle-probe method. *J. Geophys. Res.*, 64:1557–1563.

Wentworth, C. K., 1922. A scale of grade and class terms of clastic sediments. *J. Geol.*, 30:377–390.

Zoback, M. D., and Zoback, M. L., 1980. State of stress in the conterminous United States. *J. Geophys. Res.*, 85:6113–6173.

Zoback, M. L., and Zoback, M. D., in press. Tectonic stress field of the continental United States. *In* Pakiser, L., and Mooney, W. (Eds.), *Geophysical Framework of the Continental United States*. Geol. Soc. Am. Mem.

Zoback, M. D., Zoback, M. L., Mount, V. S., Suppe, J., Eaton, J. P., Healy, J. H., Oppenheimer, D., Reasenberg, P., Jones, L., Raleigh, C. B., Wong, I. G., Scotti, O., and Wentworth, C. K., 1988. New evidence on the state of stress of the San Andreas Fault. *Science*, 238:1105–1111.

Ms 125A-102